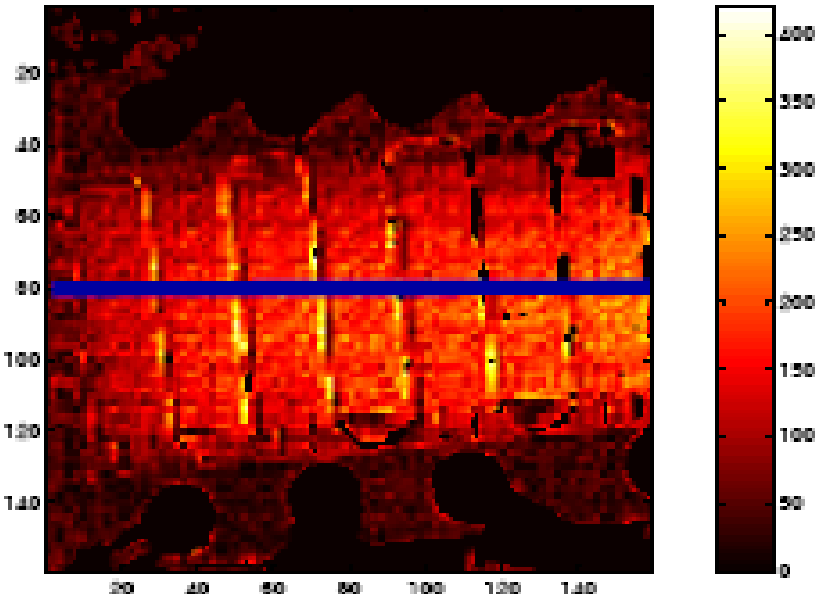


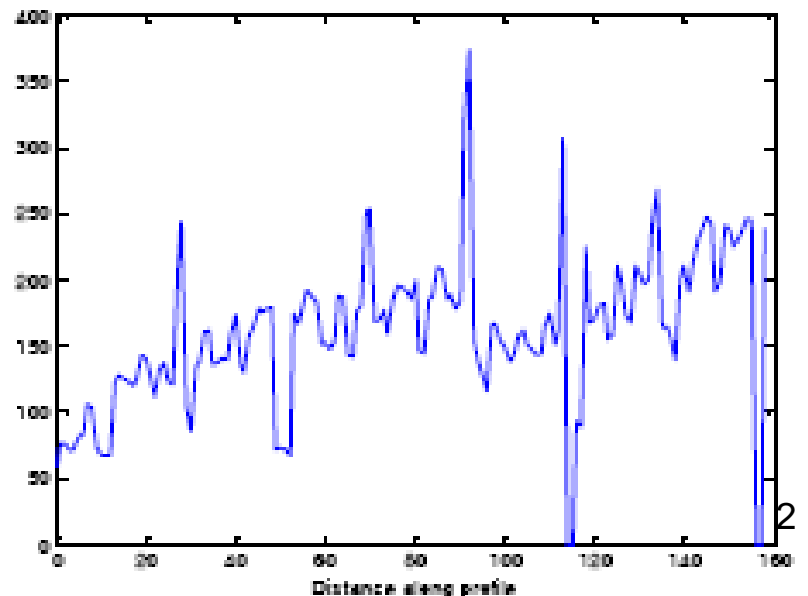
Lectures 5 - 7

**Microscale Phase Change Heat Transfer
for
Electronics cooling**

*Heat buildup is
becoming one of the
major limitations to
creating tomorrow's
more compact,
complex micro
devices".*



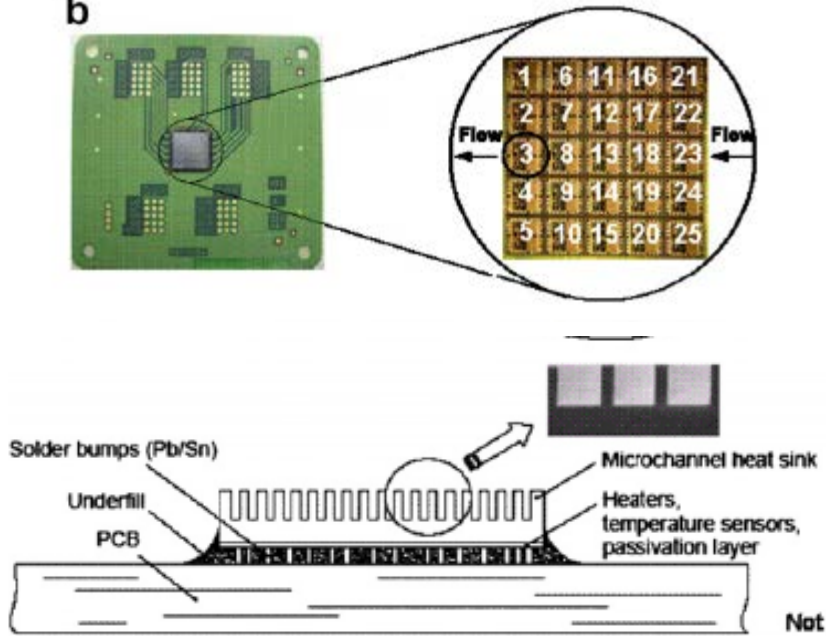
At 450 mA and 100 μ s on time and 1 KHz frequency



David Benson - Advanced
Packaging Department,
Sandia National
Laboratory's.

Electronics Cooling

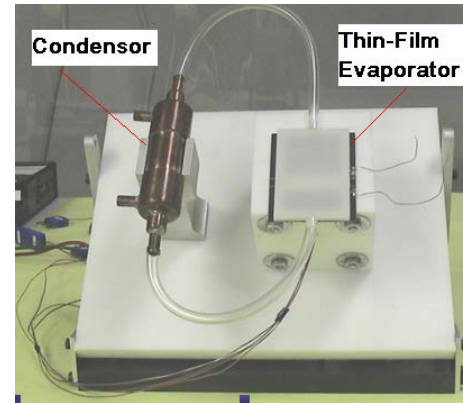
b



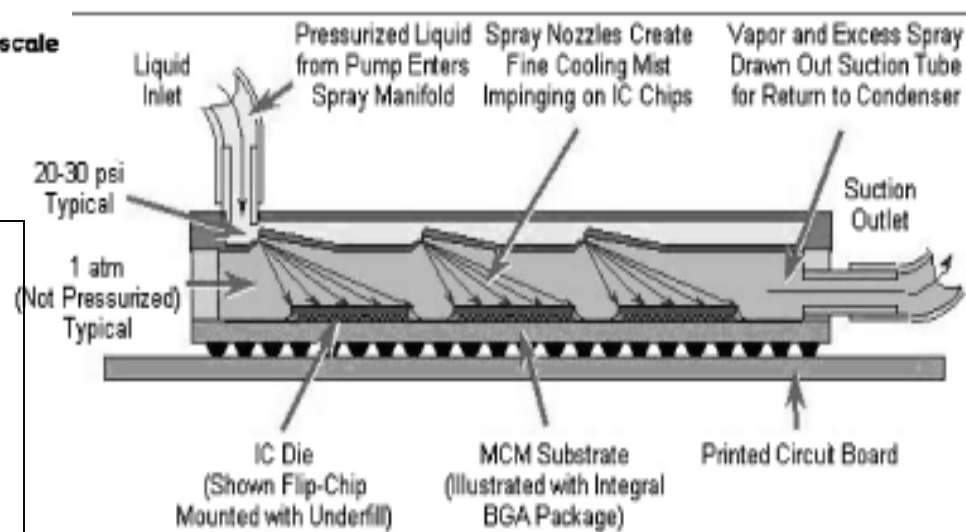
1. Micro Heat sink

- Growing demand for cooling systems
- *high heat flux removal* .
- Convection - *single phase flows* not sufficient
- *Phase change* for high heat removal

$$h_{LV} \gg C_P$$

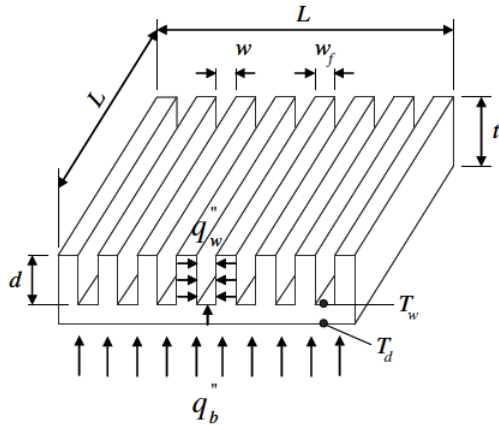


2. Thin Film evaporator

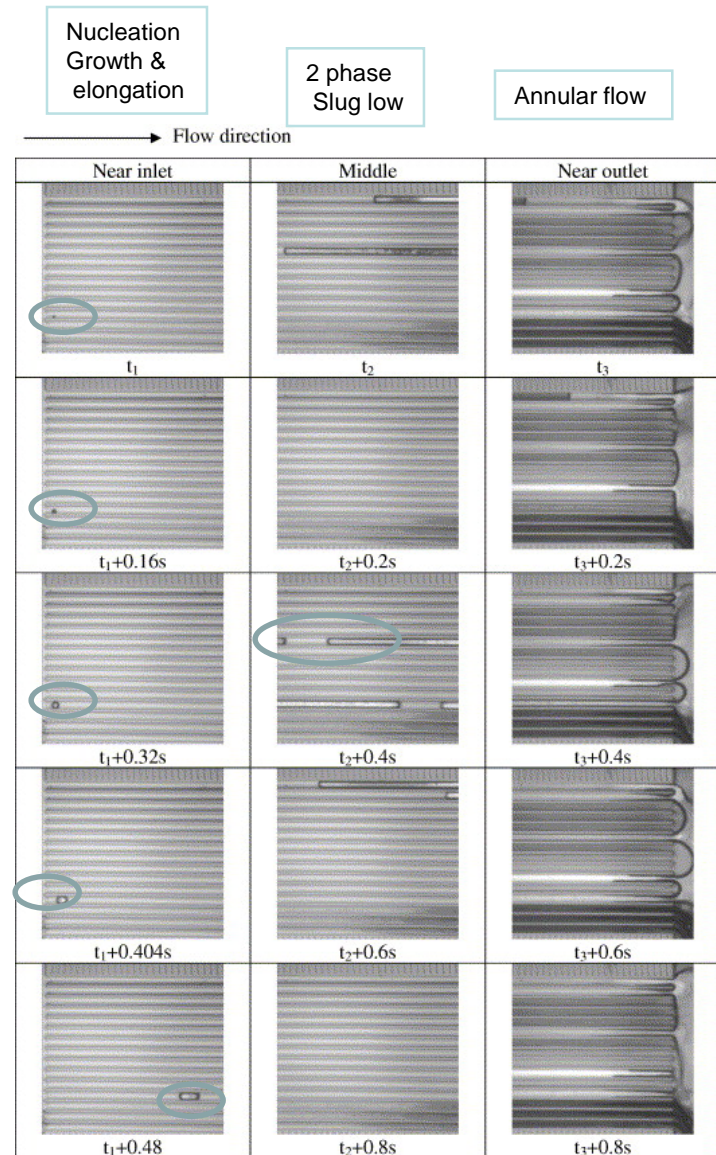


3. Spray Cooling

1. Micro Heat sink

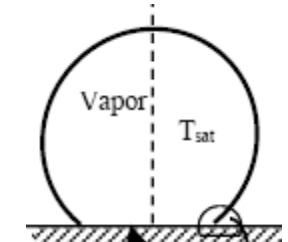
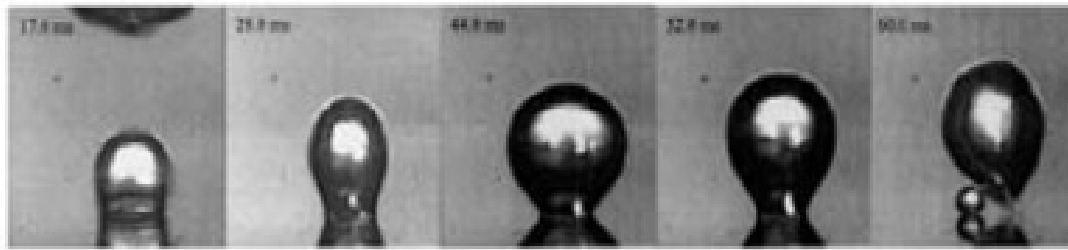


- Absorbs heat generated by electronic components (300 W/cm^2)
- Microchannels of various shapes trapezoidal, triangular rectangular
- Mechanism: Boiling in the microgrooves
Nucleation: formation of vapor bubbles
Two Phase Flow : Growth and Elongation of bubbles to form slug flow and finally annular flow



Source : Chang (2007) Two-phase flow instability for boiling in a microchannel heat sink [International Journal of Heat and Mass Transfer, Volume 50, Issues 11-12, June 2007, Pages 2078-2088](#)

Nucleation in microchannels



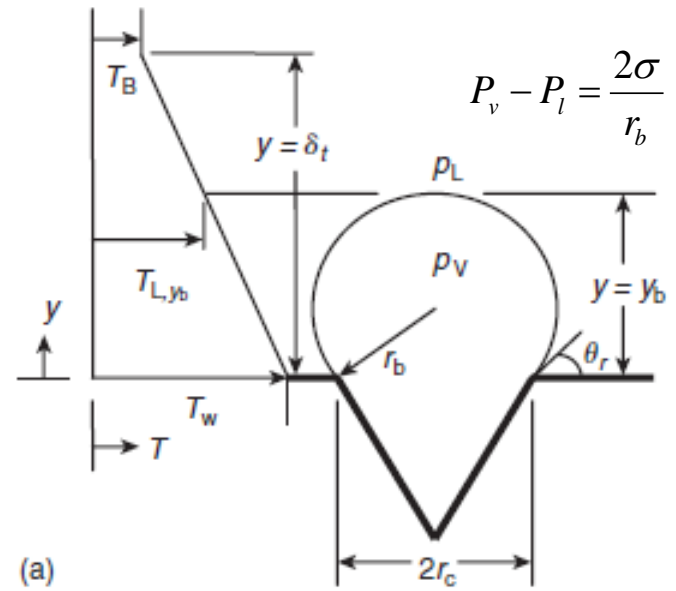
Source: Mukherjee, A. and Kandlikar, S. G., Numerical study of growth of a vapor bubble during flow boiling of water in a microchannel, ASME Paper No. ICMM 2004-2382, in *Proceedings of the Second International Conference on Microchannels and Minichannels 2004, Rochester, New York*, pp. 565–572, 2004

- Crevices serve as *nucleation sites*
- Wall superheat required for nucleation to occur on crevice of radius r_c

$$\Delta T_{Sat|ONB \text{ at } r_c} = \frac{1.1r_c q''}{k_L \sin \theta_r} + \frac{2\sigma \sin \theta_r}{r_c} \frac{T_{Sat}}{\rho_V h_{LV}}$$

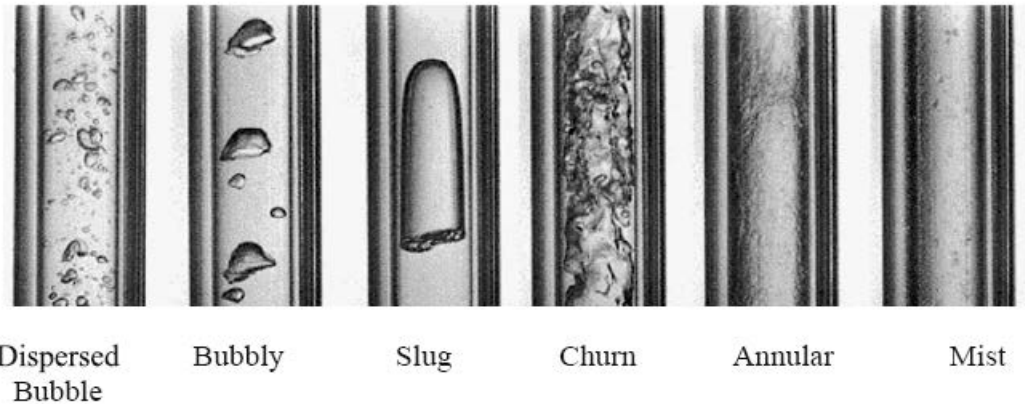
where

$$\Delta T_{Sat} = T_w - T_{Sat}$$



Source: Kandlikar, S. G. and Spiesman, P. H., Effect of surface characteristics on flow boiling heat transfer, Paper presented at the Engineering Foundation Conference on Convective and Pool Boiling, May 18–25, Irsee, Germany, 1997.

Microchannel Two Phase flows

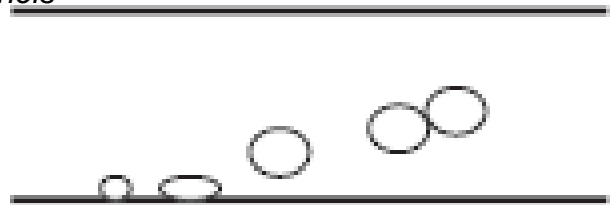


Source: Huo, X., Chen, L., Tian, W. and Karayannidis, T., (2003) Flow boiling and flow regimes in small diameter tubes, 8th UK National Heat Transfer Conference, Oxford, September 2003, Paper No.

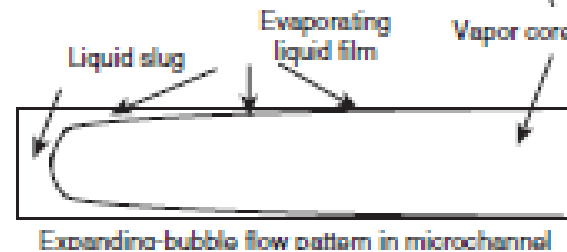
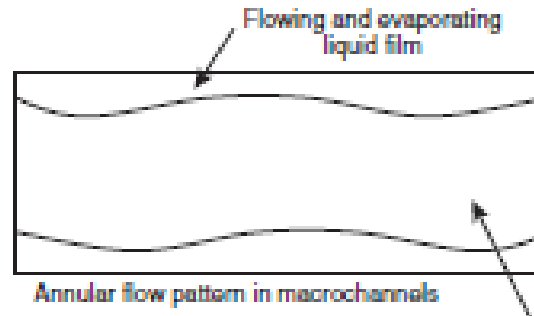
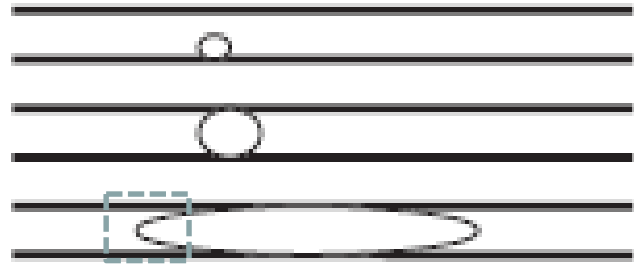
Dimensionless no	Expression	Relevance
Bond or Eötvös no	$Bo = \frac{g(\rho_l - \rho_v)L^2}{\sigma}$	Ratio of gravity force to surface tension
Capillary no	$Ca = \frac{\mu V}{\sigma}$	Ratio of Viscous to surface tension forces
Weber no	$We = \frac{LG^2}{\rho\sigma}$	Ratio of inertia to surface tension forces G = mass flux = ρV
Jacob no	$Ja = \frac{\rho_L}{\rho_V} \frac{c_{p,L}\Delta T}{h_{LV}}$	Ratio of Sensible heat for reaching T_{sat} to the latent heat

Comparison of flow boiling in Macro and Microchannel

Macrochannels



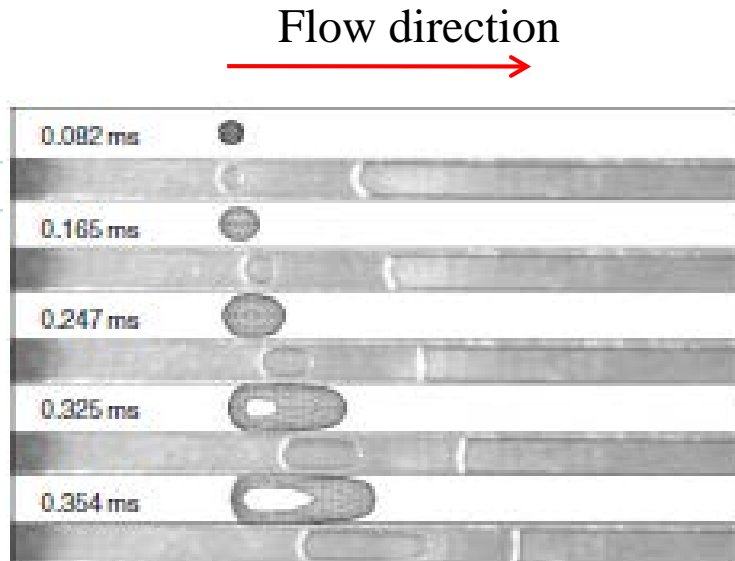
Microchannels



- *Macrochannels* : Bubbles grow in size and depart due to inertia of flow contributing to bubbly flow. When the bubble coalesce they form *bubbly* and *annular flows*.
- *Microchannels* : Bubbles grow and hit the walls and spread over the channel wall. Flow pattern similar to film under a growing vapor bubble. *Strong dependence of heat transfer coefficient* during flow boiling in microchannels indicating dominance of *nucleate boiling* .

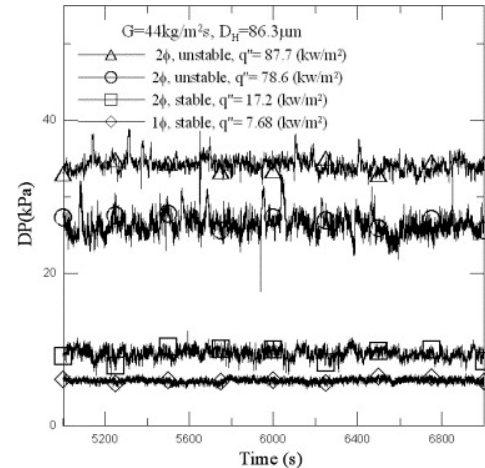
Flow Instability due to growing Bubbles

Simulation
Experimental

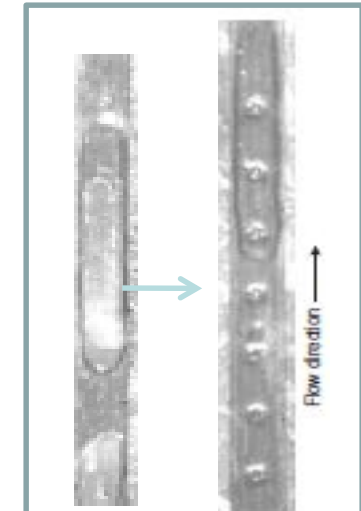


*Source :Mukherjee, A. and Kandlikar, S. G., Numerical study of growth of a vapor bubble during flow boiling of water in a microchannel, ASME Paper No. ICMM 2004-2382, in *Proceedings of the Second International Confer. on Microchannels and Minichannels 2004, Rochester, New York, pp. 565–572, 2004*

- Growth of bubble and their expansion causes *flow reversal* leading to instability - a major concern for flow boiling .
- Two methods for reducing instability
 - Pressure drop element* at the inlet
 - Flow stabilization with artificial *nucleation sites*



Pressure fluctuation



Stabilized flow with fabricated nucleation sites

2. Ultra Thin Film evaporation cooling

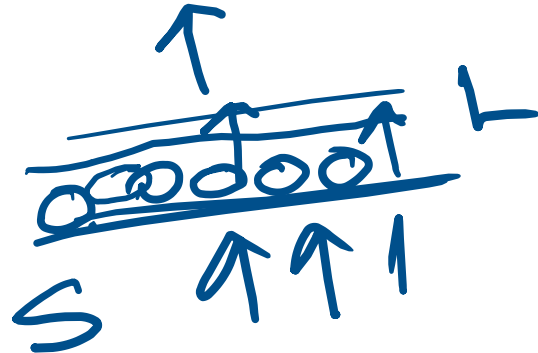
- During Phase change heat transfer, heat is absorbed by the working fluid as *heat of vaporization* or latent heat.
- Two main regimes of phase change for cooling are:
→ *boiling* and *thin film evaporation*.
- Concerns of boiling:
 1. *minimum superheat* required for boiling inception.
 2. *relatively thick boundary layer*.
 3. *inherently low critical heat flux*.
- These limitations can be overcome if a *thin film* (several microns) of the working liquid continuously covers (*wets*) the heated surface.
- Advantages of UTF evaporation over boiling:
 1. A very *small temp rise* above saturation temperature .
 2. Unlike nucleate boiling , it is *stable* because there is only conduction across a thin film.



I

AIR

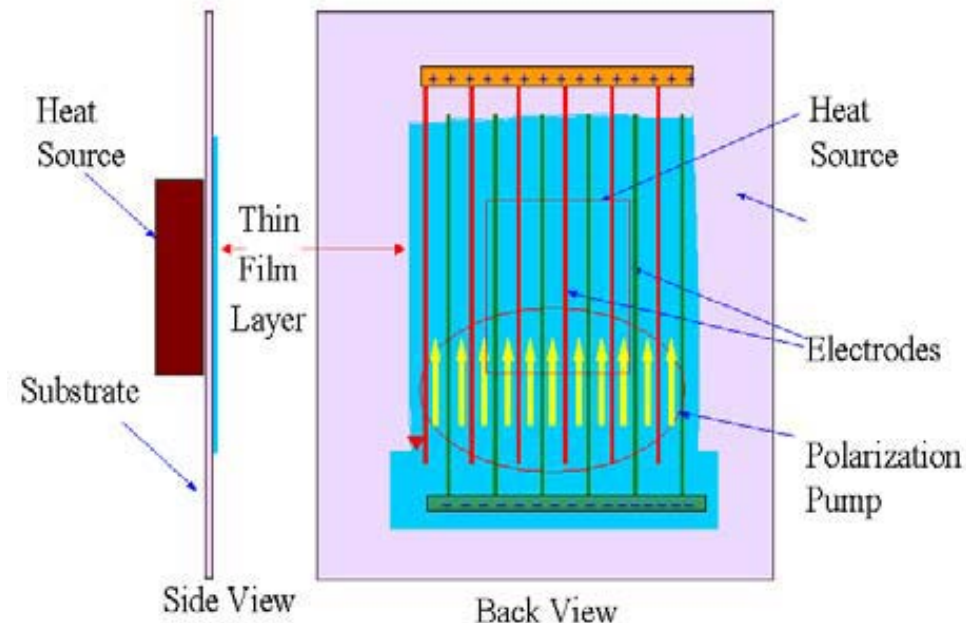
Δh



EHD enhanced polarization pump

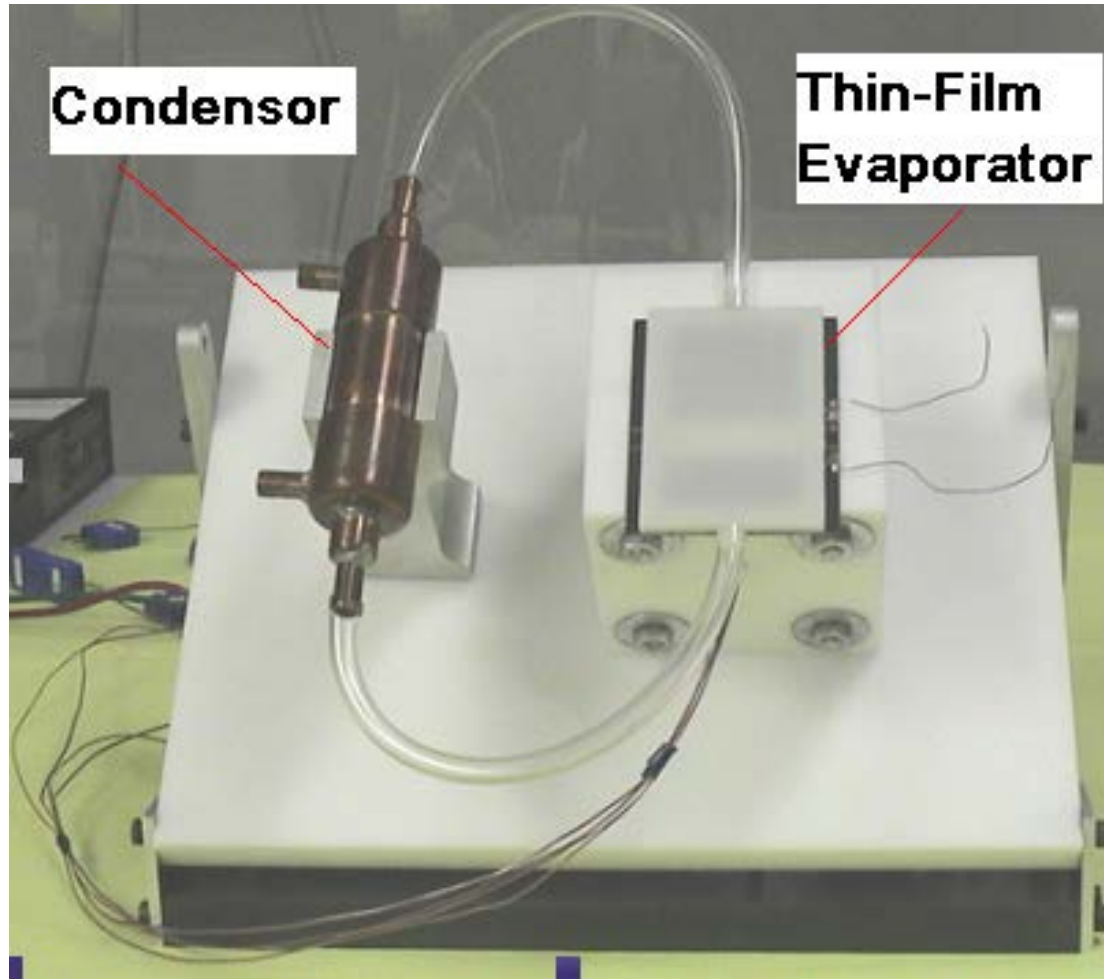
The Electrohydrodynamic (EHD) pump is a non-mechanical pump which induces flow in a dielectric liquid under a high voltage electric field by injection or generation of ions in the vicinity of the electrodes.

The free charges begin to move towards the electrode with opposite polarity. The movement of charged particles exerts a drag force on the liquid molecules resulting in a net flow along the channel.



S. Kakaç et al. (eds.), *Microscale Heat Transfer*, 321 338.
© 2005 Springer. Printed in the Netherlands.

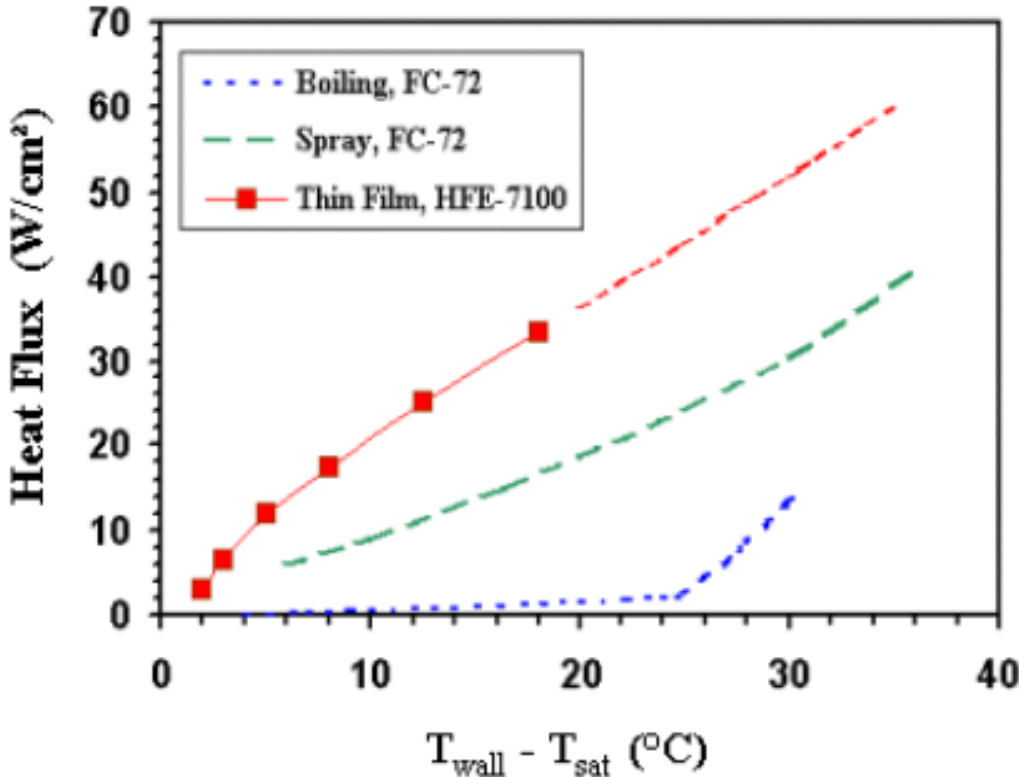
- Array of EHD electrodes draws an *ultra thin liquid film* over the hot surface.
- The power required is very low, leading to higher pumping efficiencies.



The thermosyphon test system

The ultra thin film evaporator can be packaged into a wide variety of configurations depending on the electronic components to be cooled.

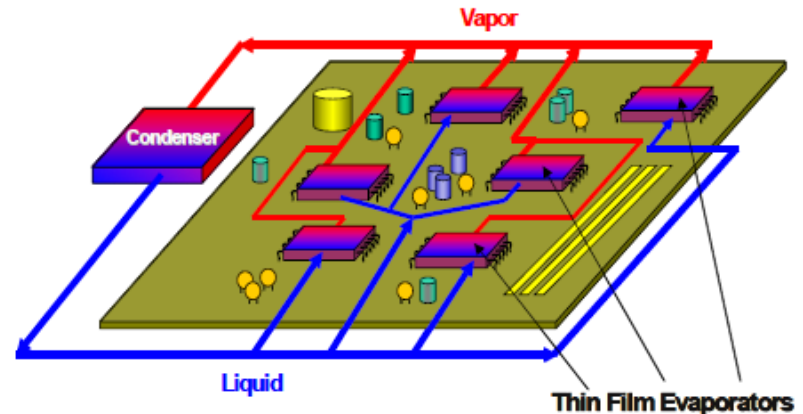
Comparison of boiling, spray and thin film



*S. Kakaç et al. (eds.),
Microscale Heat Transfer,
321 338. © 2005 Springer..*

- The thin film evaporator can remove heat fluxes of $20-40 \text{ W/cm}^2$ with a temperature difference that is about $10-15^\circ\text{C}$ less than spray cooling and about 30°C less than pool boiling.
- Optimizing the electrode pattern on the thin-film evaporator will generate *ultra thin (micron-size) films* on evaporator surfaces, higher cooling rates, and a more robust operation.

- Cooling systems based on the ultra thin film evaporator will be *quiet, compact, light-weight*, and energy efficient.
- The high rate of cooling will minimize the *operating temperature* of the electronic components being cooled.

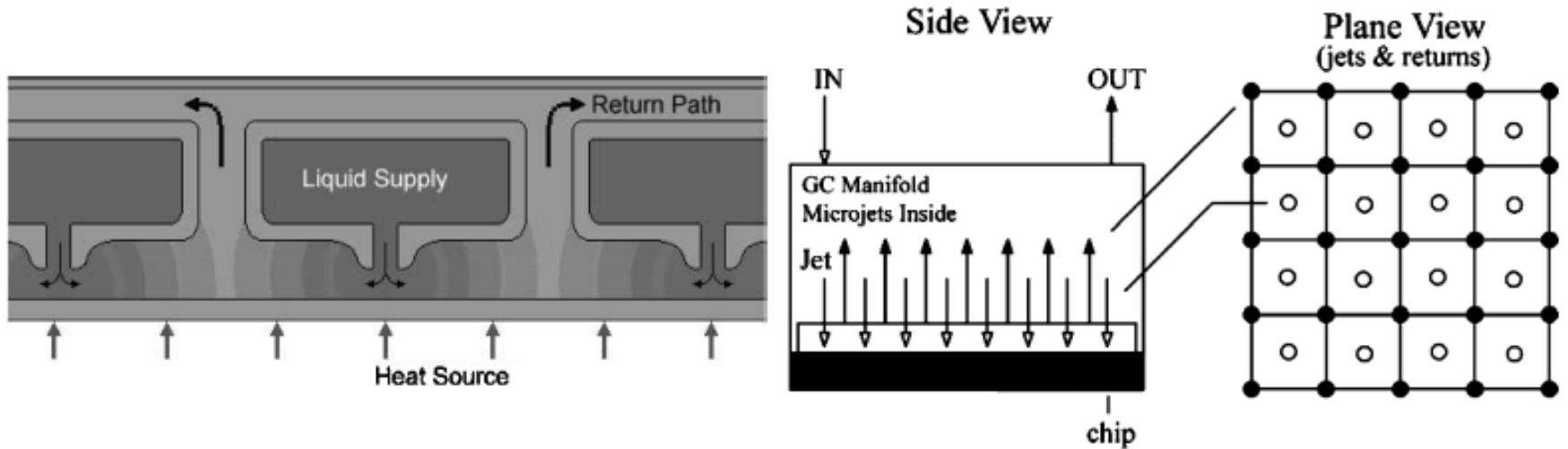


Example of thin film cooling architecture

Conclusions

- This technology can substantially increase cooling capacity and lead to major *weight/volume reductions* in the next generation thermal management systems.
- *Only a fraction of the amount of fluid* used in spray or jet cooling systems is necessary for UTF and with few ancillary components.
- Its *power consumptions* are extremely low and thus highly energy efficient for cooling of high heat-flux devices.

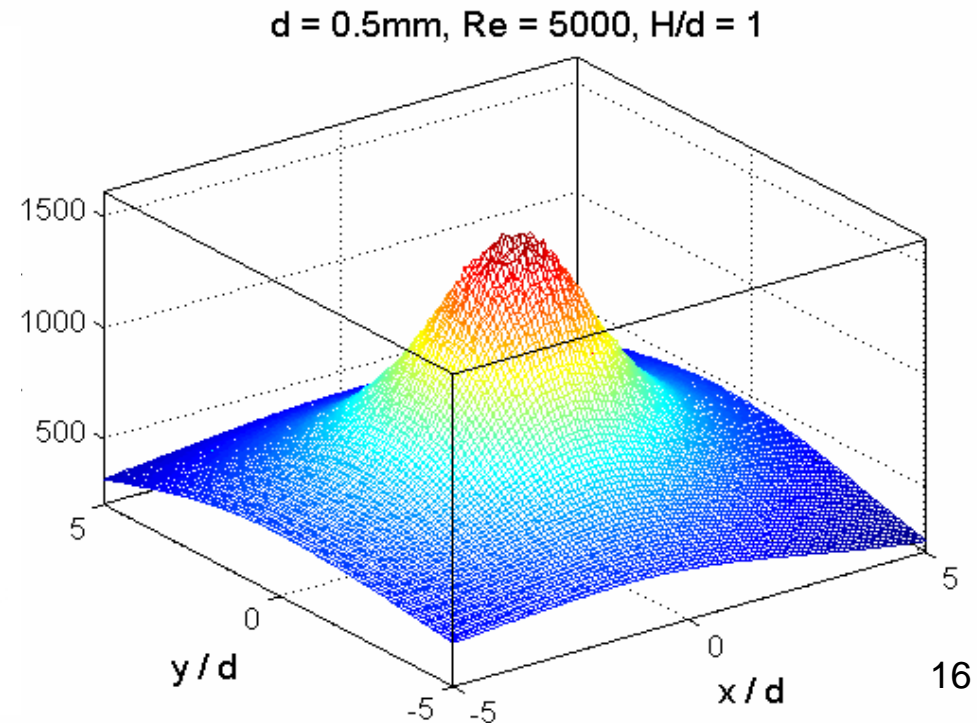
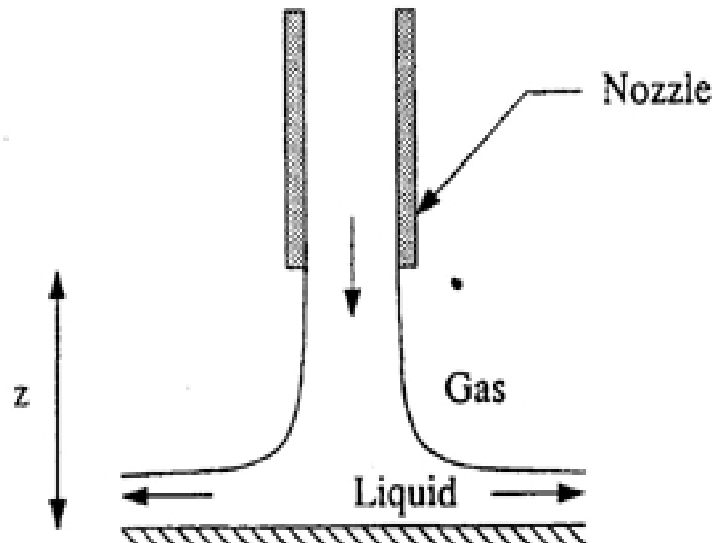
3. Microjet Impingement Cooling



- Applications: Plasma, optical beams, Semiconductor Laser Arrays
- *High Speed jets* from nozzles hit target , flow radially and return.
- *Very Thin Boundary Layer* is formed under the jet and high heat transfer coefficient
- Multiple nozzles to maintain temperature uniformity.

Basics

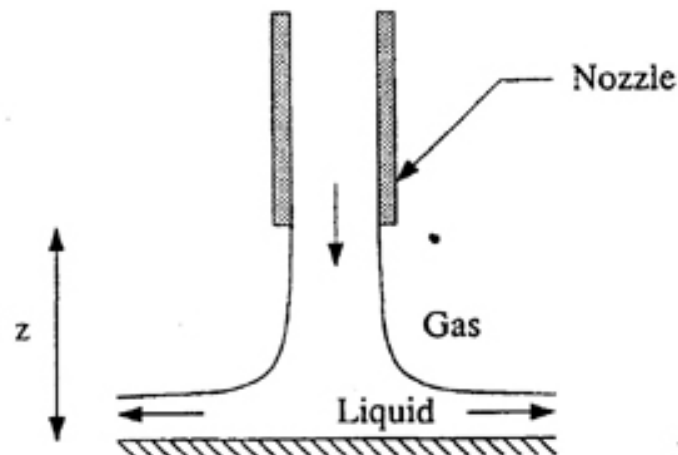
- A *high speed jet* issue from nozzles and impinge on the target plate.
- The main reason for *high heat transfer coefficient* of around 250W/cm^2 is that a very *thin boundary layer* is formed under the jet.
- As fluid start flowing radially outward the boundary layer thickens, and heat transfer is adversely affected.



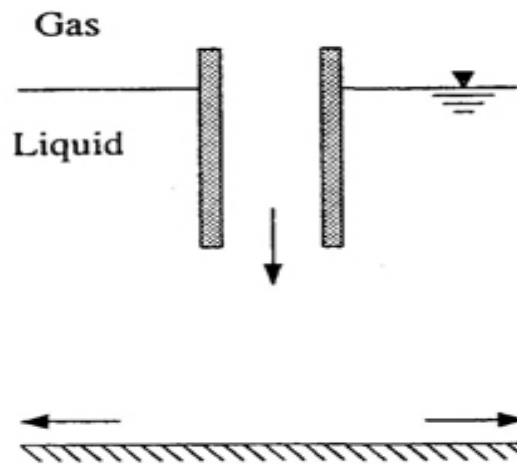
Types of Jet Impingement

1. *Free Jet Impingement.*
2. *Submerged Jet Impingement.*

- Heat transfer coefficient for the system is a complex function of many parameters like Prandtl No, Reynolds No, nozzle to plate spacing, displacement from the stagnation point etc.



Free Jet Impingement.



Submerged Jet Impingement.

Characteristics: Advantages and disadvantages

Advantages

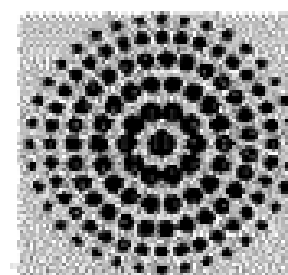
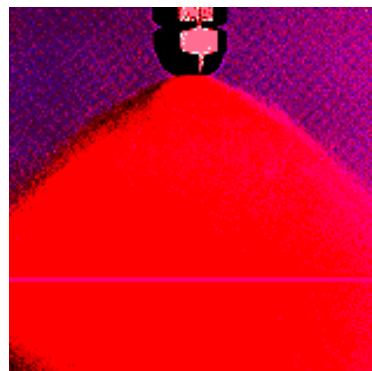
- Under Nucleate Boiling Mode: increased bubble departure frequency and *higher heat transfer coefficient*
- Offers good solution for localized cooling.

Disadvantages

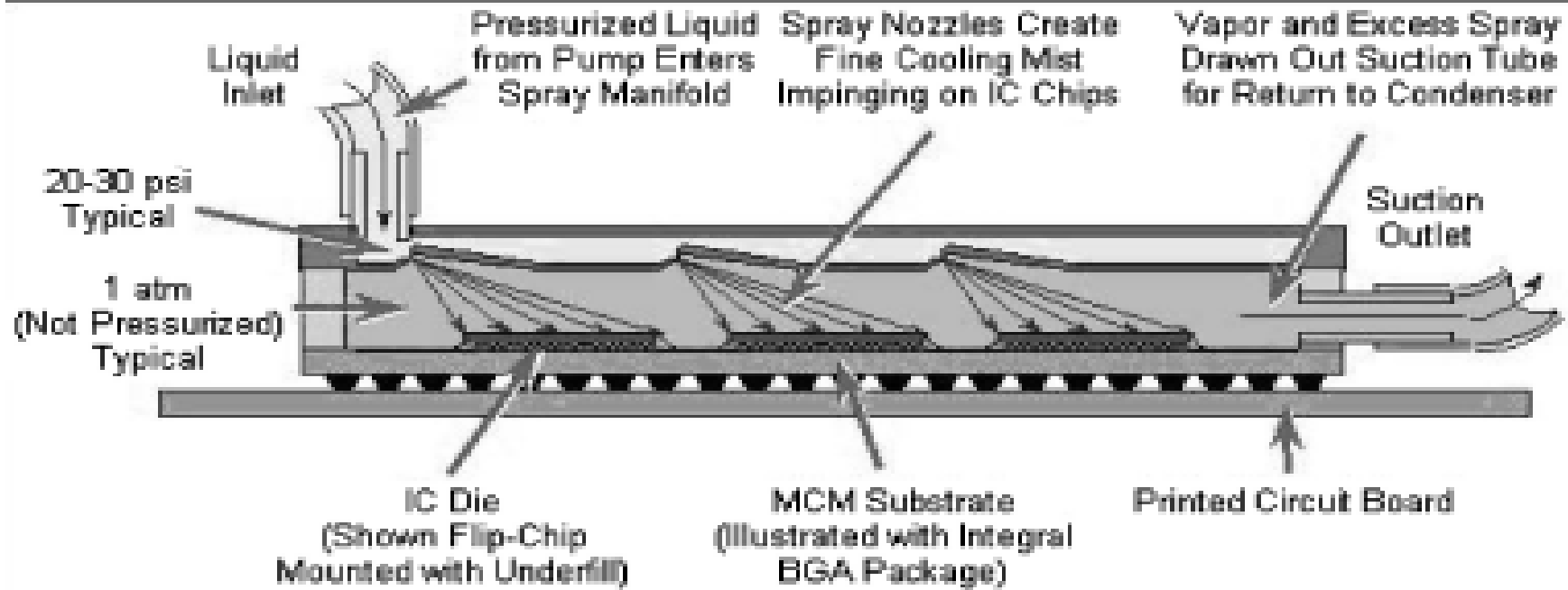
- *Multiple jets necessary.*
- Nozzle arrangement, return paths extremely important for uniform temperature distribution
- At micro-processor level cooling, management of inlet outlets, jet geometry and configuration, jet velocity parameters to be optimized

4. Spray cooling

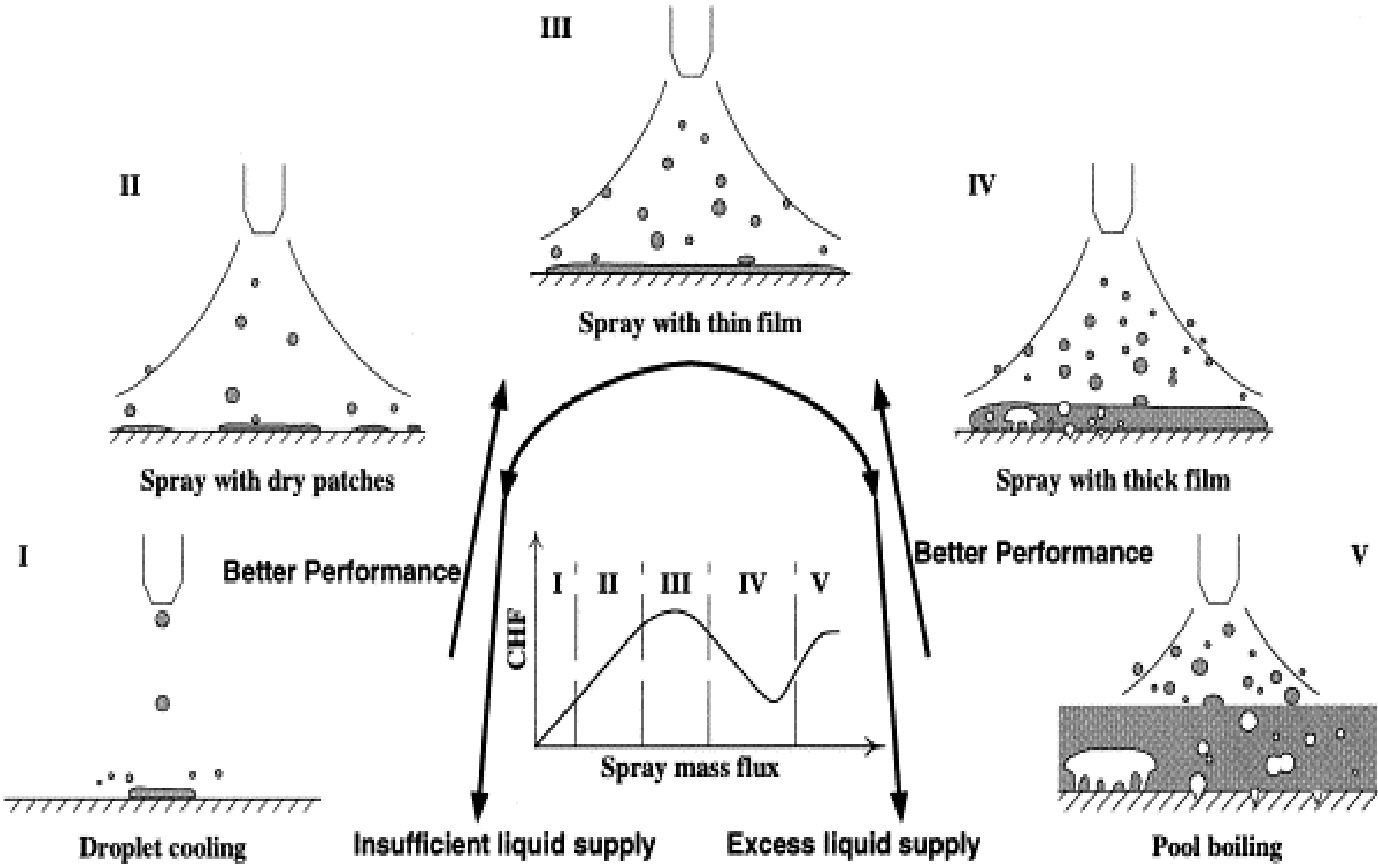
- Spray cooling occurs when liquid is forced through a small orifice, shatters into a dispersion of fine droplets, which then impact on a heated surface.
- Droplets spread on the surface and evaporate by forming **thin liquid films**.
- Dissipate large amounts of heat due to latent heat of evaporation.
- Supply of cold liquid decides the performance of cooling.
- Spray inclination angle will also affect the performance of cooling



Spray Cooling



- Liquid droplets impinge on the surface.
- Thin films are formed on the surface .
- Large heat removed by evaporation (phase change) .
- $500\text{W}/\text{cm}^2$



Characteristics: Advantages and disadvantages

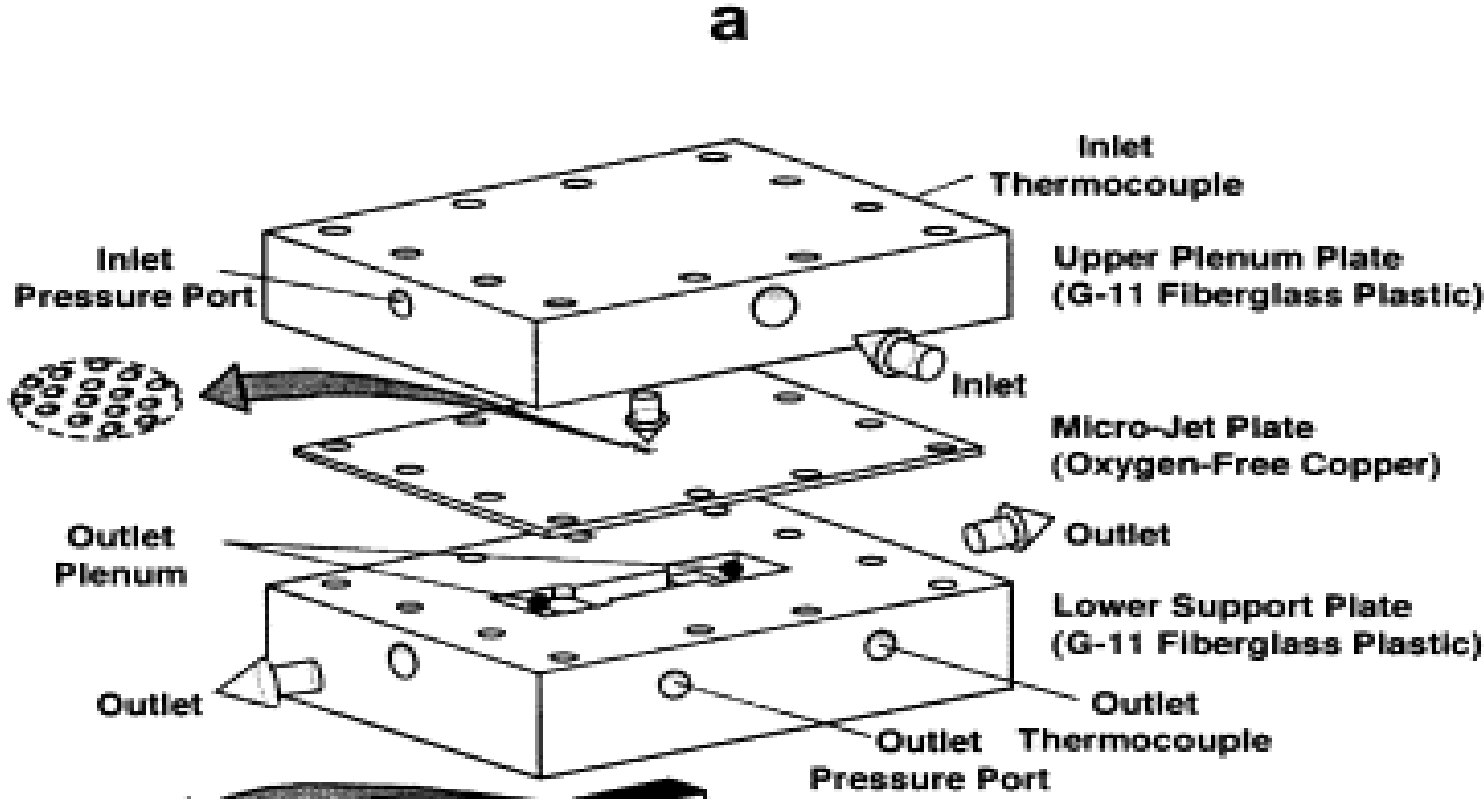
Advantages

- Possibility of uniformly cooling *larger surfaces*.
- *Less resistance* to the removal of vapor from the heated surface.

Disadvantages

- Multiple sprays necessary.
- Heat transfer is a complex function of droplet size distribution, droplet number density, velocity of liquid flow rate.
- *High Pressure drop*.

Hybrid Scheme for cooling

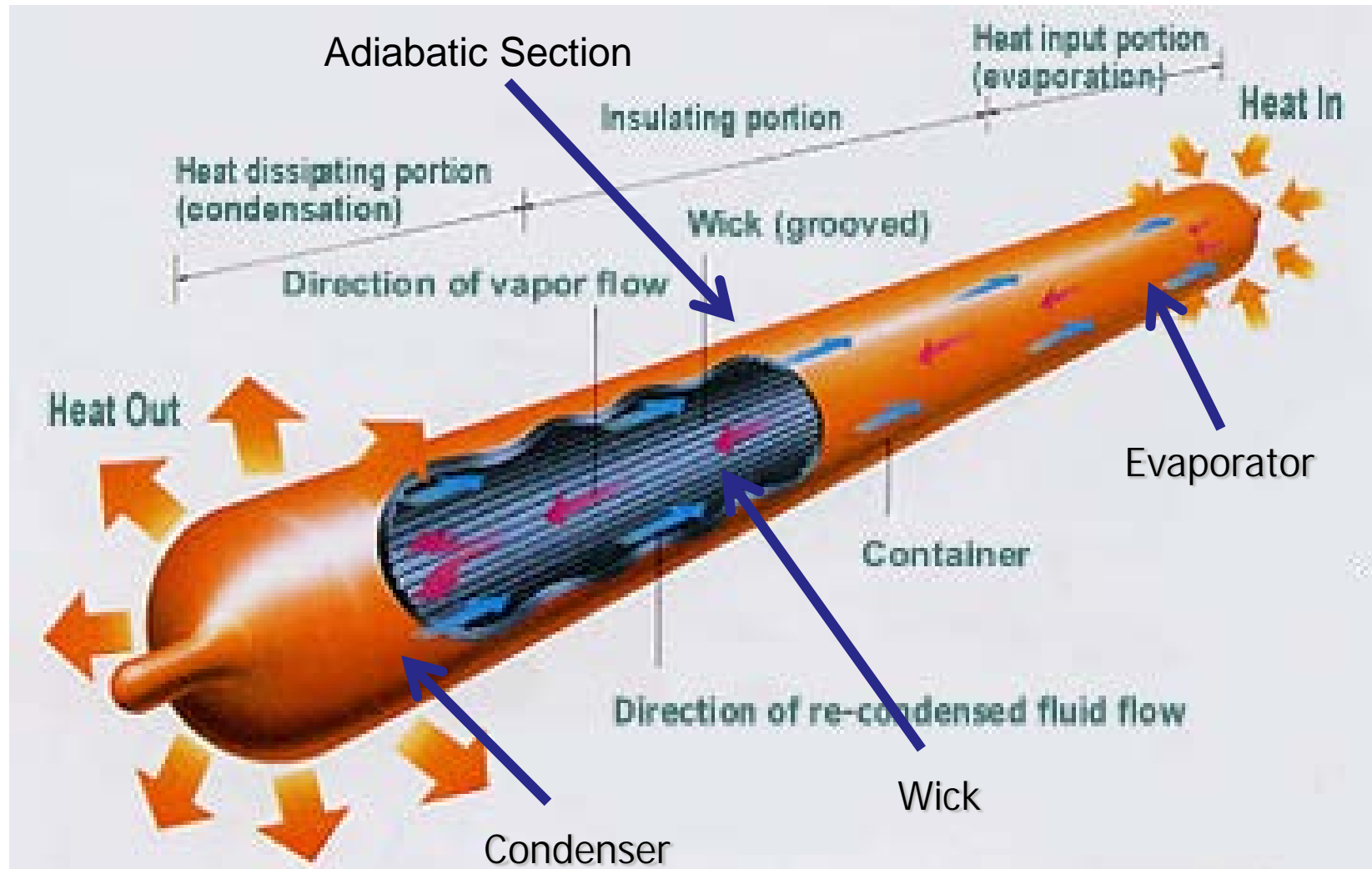


Hybrid scheme test module (high performance) 6. Schmidt, R., 2000, "Low Temperature Electronic Cooling", Electronics Cooling, Vol.6 (3), pp.18-24.

In jet impingement, problems arise due to flow blockage between closely spaced jets. It is a combination of impingement cooling and channel cooling for maintaining fairly uniform temperatures.

Heat Pipes

Evaporator - Adiabatic Section - Condenser - Liquid flow towards the evaporative section, due to capillary pumping,



Typical values of heat transfer coefficients

Description	Heat Transfer Coefficient (W/m ² K)
Natural convection, air	3-25
Natural convection, water	15-1000
Forced convection, air	10-200
Forced convection, water	50-10,000
Condensing steam	5000-50,000
Boiling water	3000-100,000
Ultra thin film evaporation	10,000-500,000
Microchannel Cooling	10,000-1,000,000

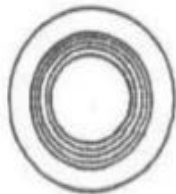
(Ref: Ohadi et al. 2005)

Advantages of Heat Pipes

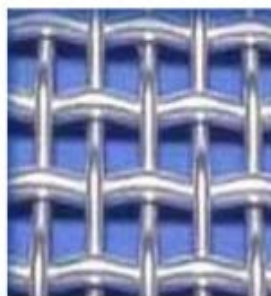
- Very high thermal conductivity. Less temperature difference needed to transport heat than traditional materials (thermal conductivity up to 90 times greater than copper for the same size) (Faghiri, 1995) resulting, in low thermal resistance.
- Efficient transport of concentrated heat. (Faghiri, 1995)
- Temperature Control. The evaporator and condenser temperature may remain nearly constant (at T_{sat}) (Faghiri, 1995) .

Types of Wicks

Screen Mesh



Wrapped Screen

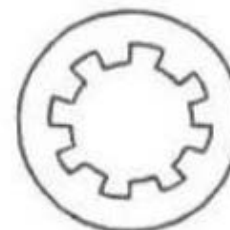


Utilizes multiple wire layers to create a porous wick.

Sintering can be used.

Axial Grooves

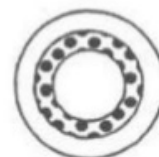
Axial Groove Wick



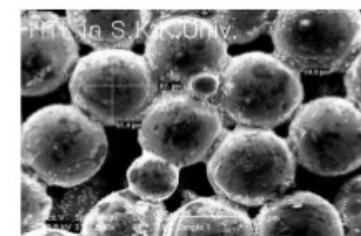
Axial Groove



Sintered Powdered Wick



Sintered Metal

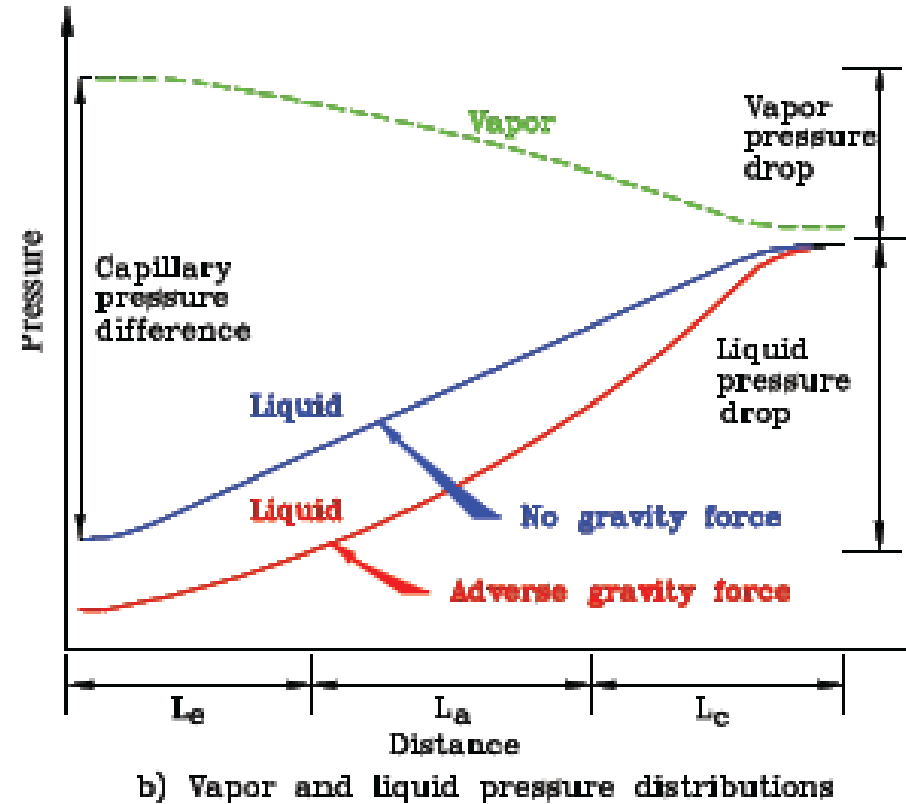
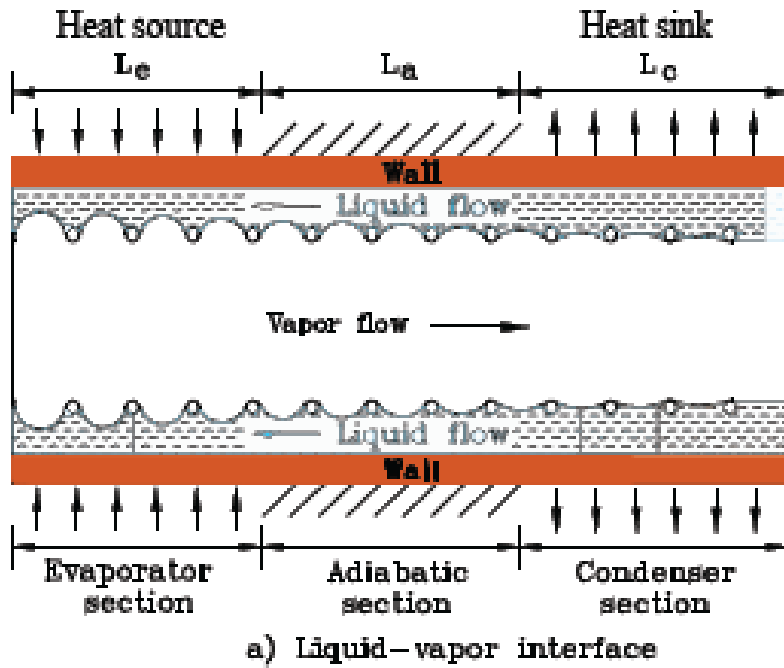


Utilizes densely packed metal spheres.

Sintering must be used to solidify the spheres²⁷

Desired Characteristics of a Heat Pipe & Coolant

- Compatibility of the coolant with the wick and the heat pipe material
- Wettability
- Low liquid and vapor viscosities
- Thermal stability
- High latent heat
- High thermal conductivity
- Surface tension – high or low?



Axial variation of the liquid-vapor interface and the vapor and liquid pressures along the heat pipe

Characteristics of pressure drops in Heat Pipes

Vapor pressure changes along the heat pipe - due to friction, inertia, evaporation (blowing) and condensation (suction)

Liquid pressure changes mainly due to friction

Liquid vapor interface is flat near the condenser end-cap (zero local pressure gradient) at very low vapor flow rates

Maximum pressure difference occurs near the evaporator end-cap. This maximum local capillary pressure is equal to the sum of the pressure drops in the vapor and the liquid across the heat pipe in the absence of body forces.

If body forces are present, the liquid pressure drop is greater.

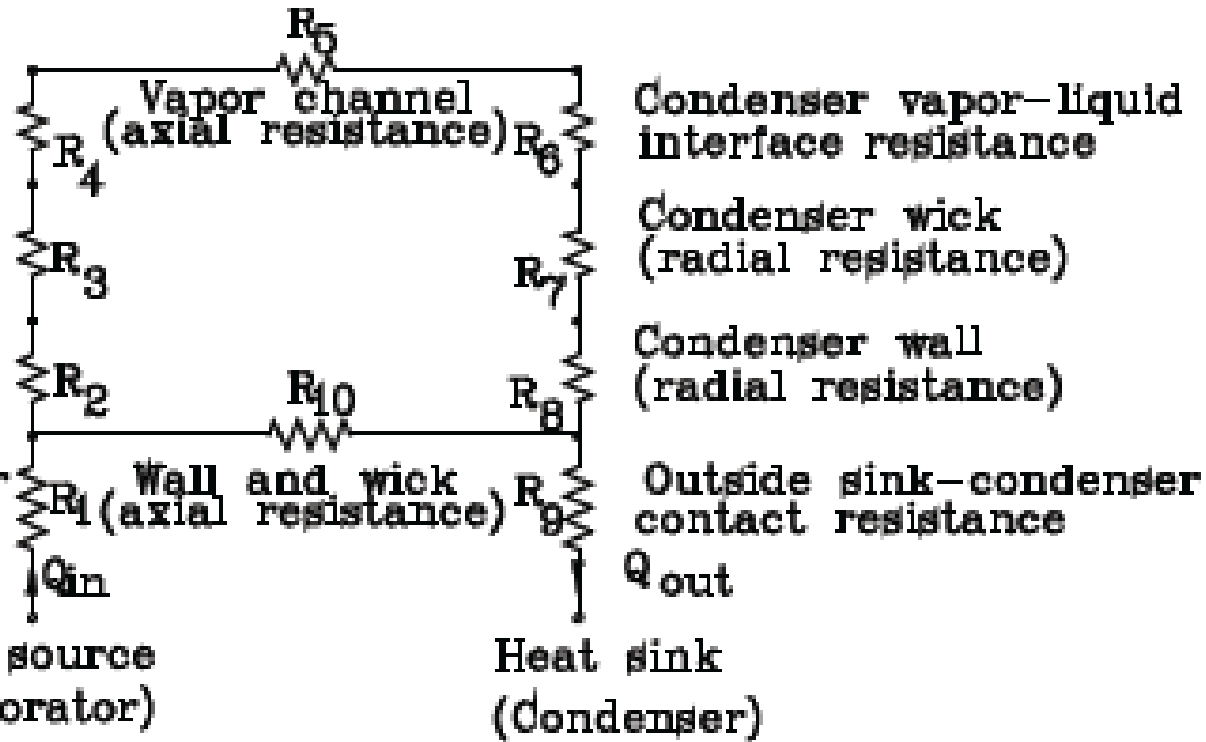
At moderate vapor flow rates, dynamic effects cause the vapor pressure drop and recovery along the condenser section.

Evaporator liquid-vapor interface resistance

Evaporator wick (radial resistance)

Evaporator wall (radial resistance)

Outside source-evaporator contact resistance



Thermal resistance model of a typical heat pipe

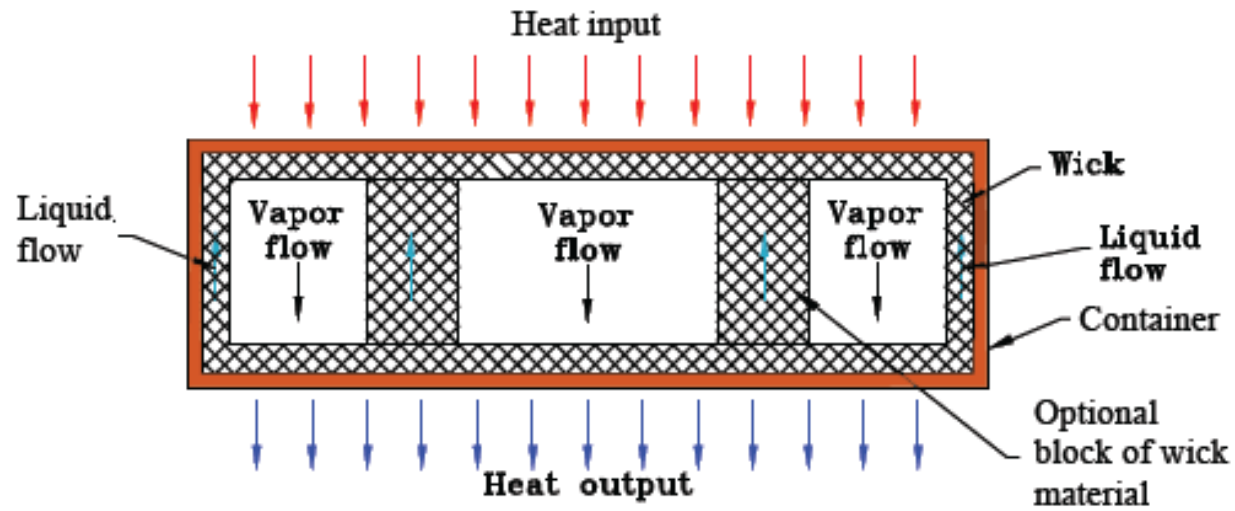
Heat Pipe Applications

- Electronics cooling - small high performance components cause high heat fluxes and high heat dissipation demands. Used to cool transistors and high density semiconductors.
- Aerospace - cool satellite solar array during reentry (ISRO uses ammonia heat pipes).
- Heat exchangers- power industries use heat pipe heat exchangers as air heaters on boilers.
- Other applications - production tools, medicine and human body temperature control, engines and automotive industry.

Types of Heat Pipes

Flat Plate

Rectangular. Used to cool semiconductor or transistor packages assembled in arrays on the top of the heat pipe.

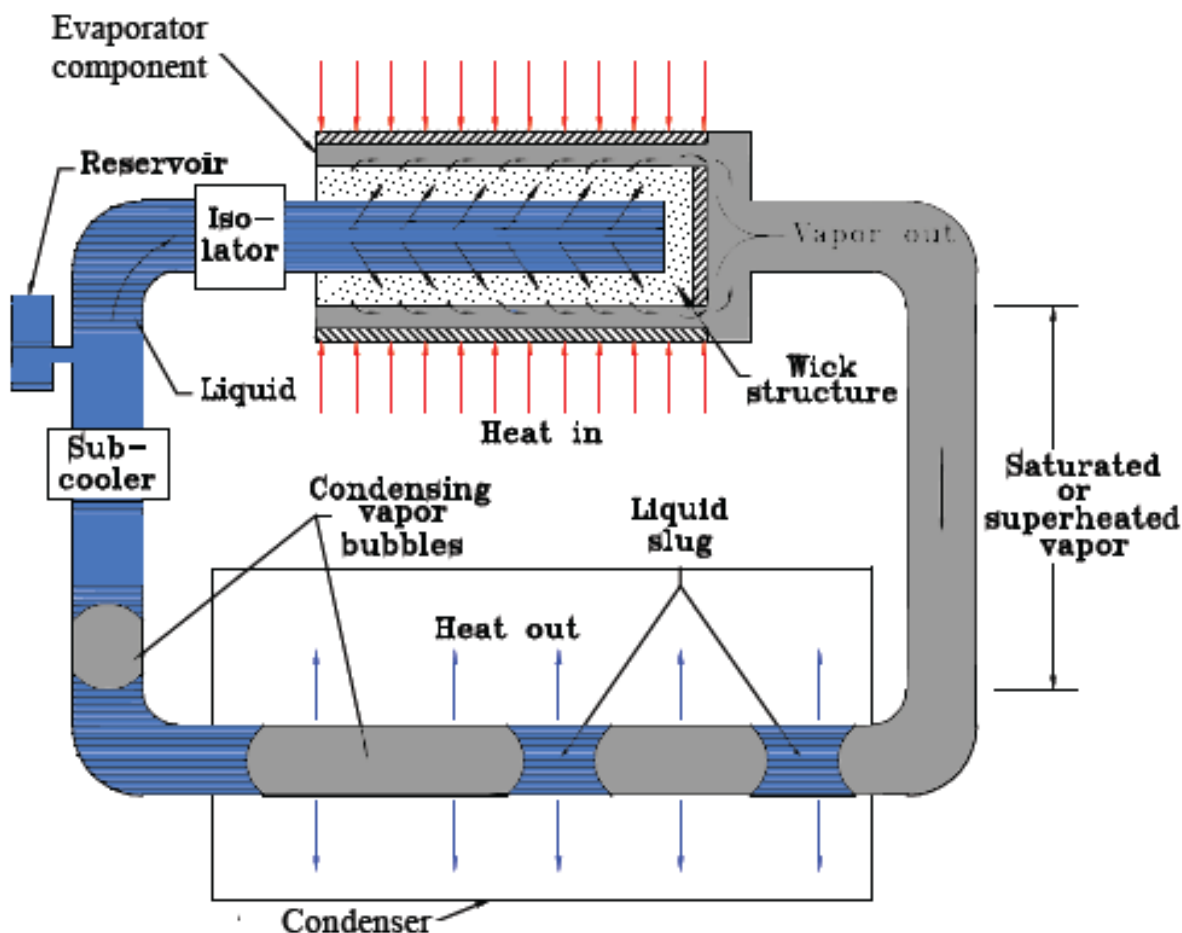


Types of Heat Pipes

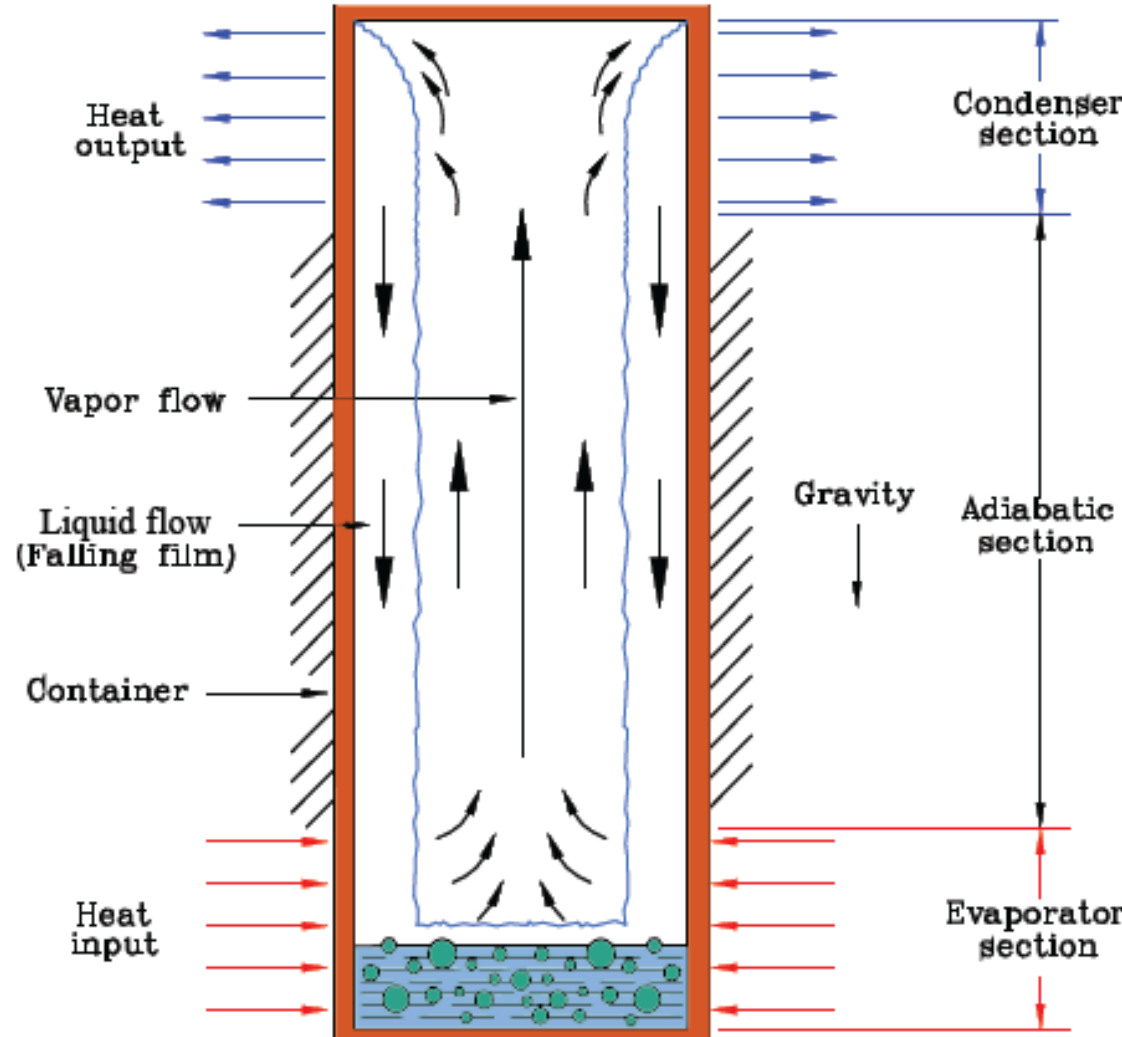
Capillary pumped loop heat pipe

For systems where the heat fluxes are very high or where the heat needs to be moved far away. The vapor travels in a loop where it condenses and returns to the evaporator.

Used in electronics cooling.



Types of Heat Pipes

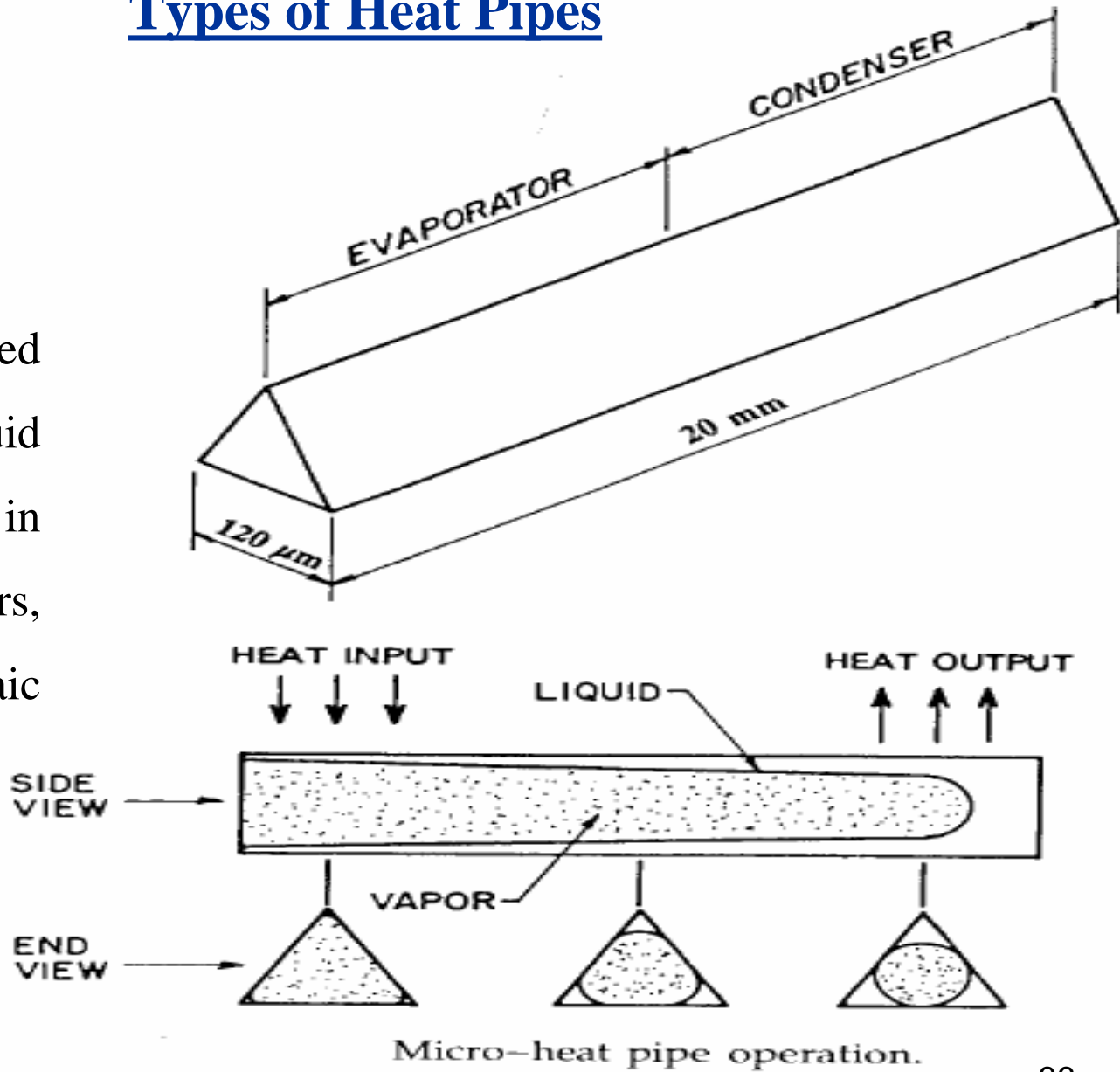


Gravity assisted wickless heat pipe (two phase closed thermosyphon)

Types of Heat Pipes

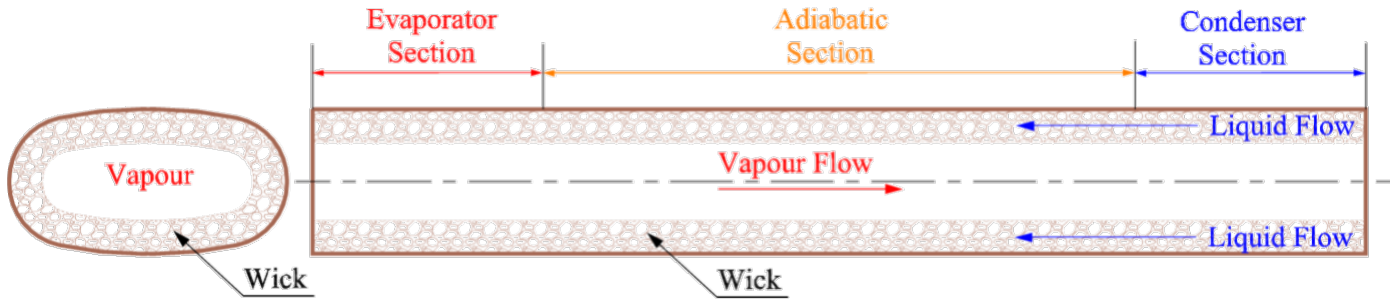
Micro heat pipes

Noncircular, angled corners act as liquid arteries. Employed in cooling semiconductors, laser diodes, photovoltaic cells, medical devices.

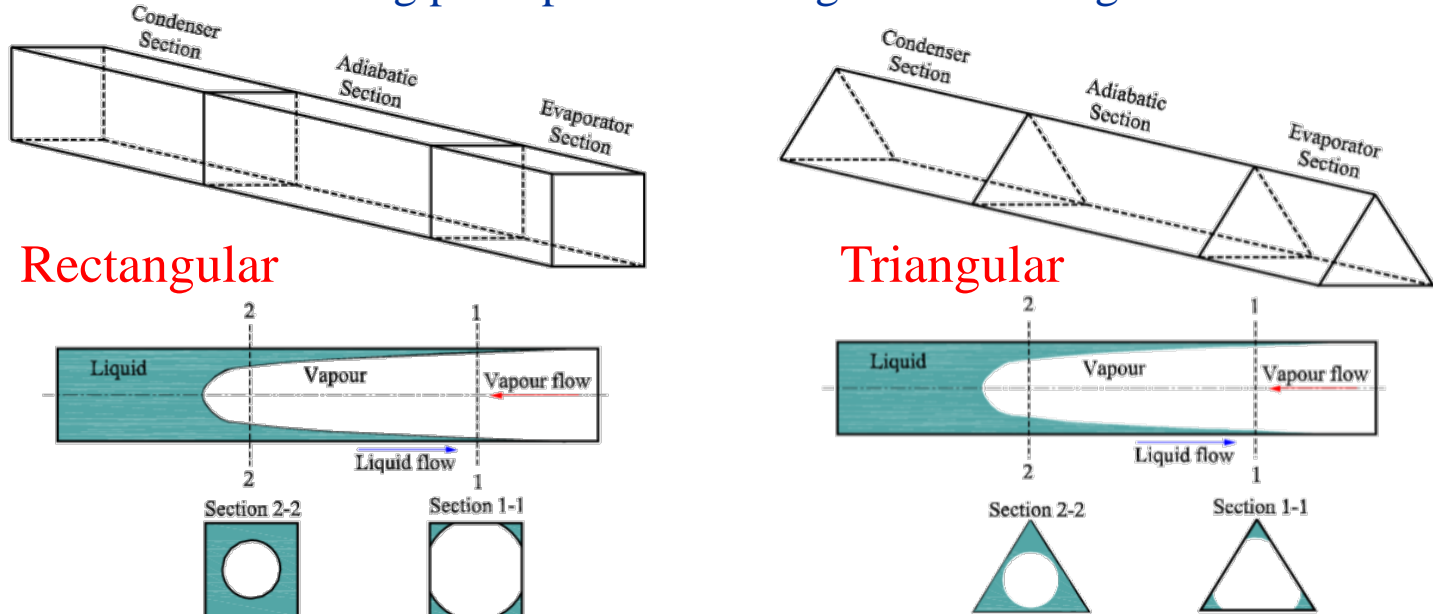


Conventional vs. Micro Heat Pipe

Schematic representation of working principle of a conventional (wicked) heat pipe



Schematic representation of working principle of a rectangular and triangular micro heat pipes

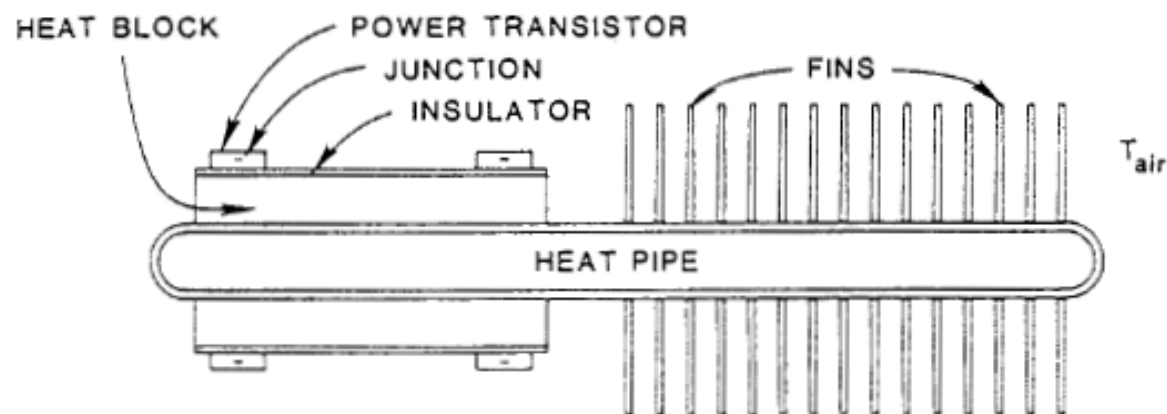


Heat Pipes in Electronics Cooling

- Common heat pipes used in electronics cooling:
 - Micro heat pipes
 - Capillary looped heat pipes
 - Flat plate heat pipes
 - Variable conductance heat pipes

Heat Pipes in Electronics Cooling

- The heat pipe's evaporator may be attached to a heat source (chip or power transistor).
- The condenser is attached to a heat sink to dissipate the heat through free or forced convection.

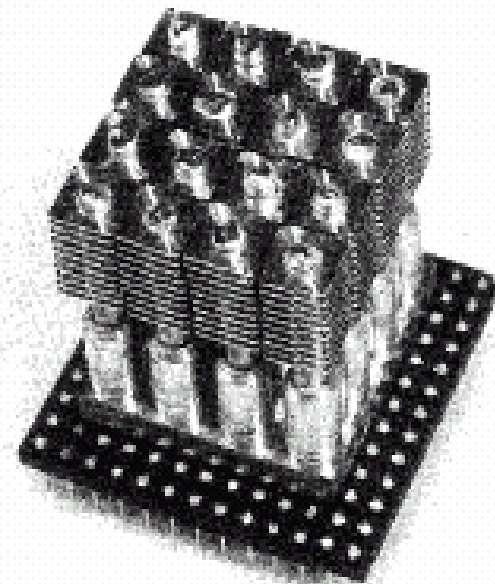


Heat pipe heat sink for power transistors (Murase et al., 1982).

Heat Pipes in Electronics Cooling

Micro heat pipes may be used for cooling individual semiconductors or an array.

Good for applications where space is limited like laptops.



Micro heat pipe array (courtesy of Itoh Research

Heat Pipes in Electronics Cooling

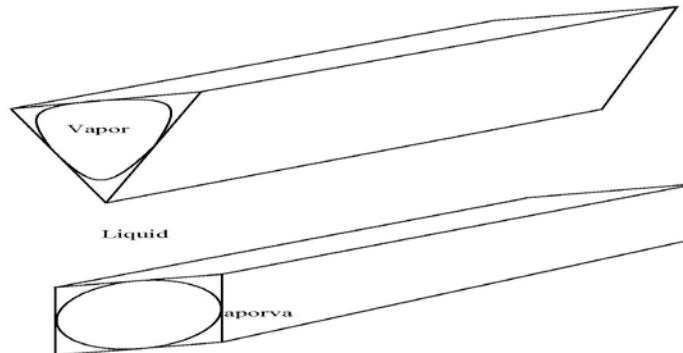
- Summary:
 - Heat pipes enable devices with higher density meet heat dissipation requirements with greater reliability.
 - Proven alternative to conventional methods

Micro Heat Pipes

A micro heat pipe is a **wickless, non-circular channel** with a diameter of 10–500 μm and a length of 10–20mm

A micro heat pipe is "so small that the mean curvature of the liquid-vapor interface is comparable in magnitude to the reciprocal of the hydraulic radius of the total flow channel" - Cotter, 1984.

The fluid flow inside the pipe is caused by **change in pressure** (due to changes in capillary and intermolecular force field) along the length of the heat pipe.



High efficiency,
reliability and cost
effective

Schematic of triangular and rectangular heat pipes

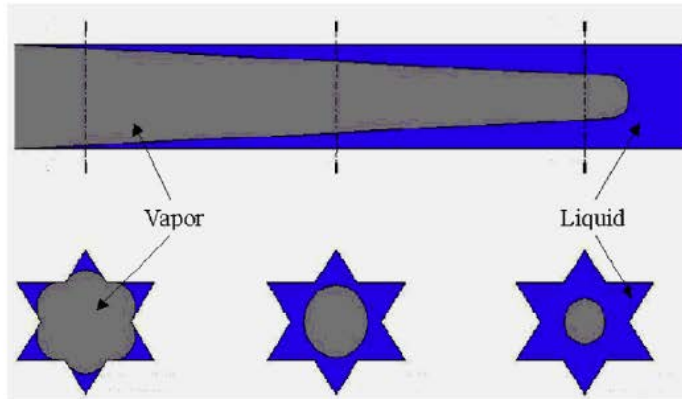
Basic Mechanisms of Transport in MHP

The net capillary force is generated by the integral effect of the evaporating and condensing menisci.

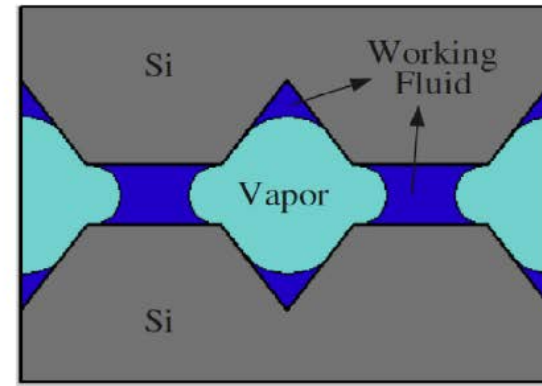
The surface tension forces, wettability and the solid–liquid interactions primarily govern the behavior of the various interfaces, particularly the liquid–vapor interface.

The fluid flow in the evaporating meniscus results from a change in the meniscus profile

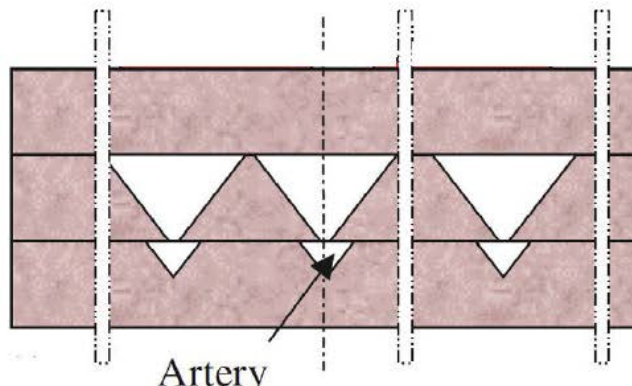
- Flow due to a difference in curvature
- Evaporation from ultrathin films where intermolecular forces predominate



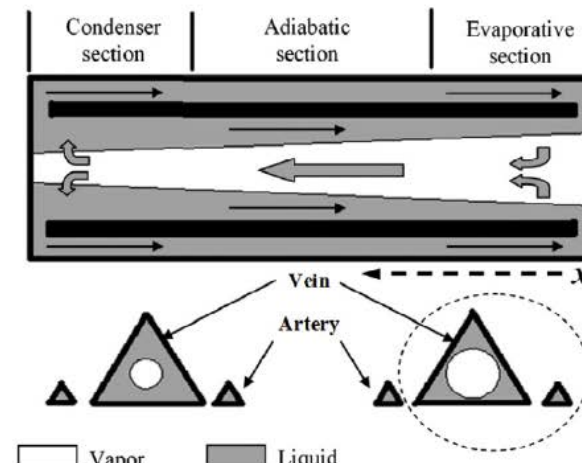
(a)



(b)



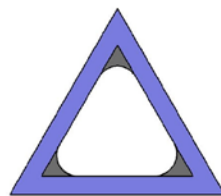
(c)



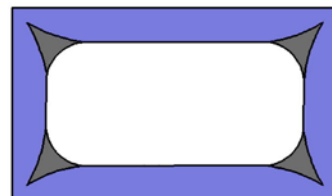
(d)

Schematic diagram of micro-GHPs with diverse novel channel structures to enhance capillarity: (a) star grooves micro-GHP (b) rhombus grooves micro-GHP; (c) triangular channels coupled with arteries (d) micro-GHP with vein and two neighboring arteries

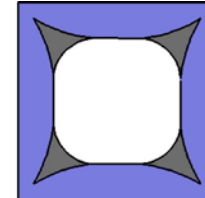
Cross sections of individual MHPs



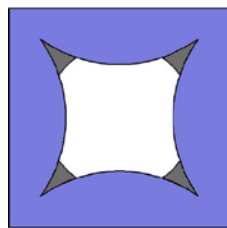
(a)



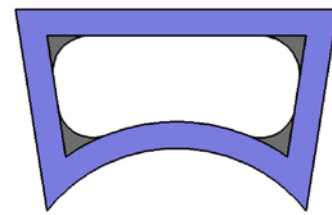
(b)



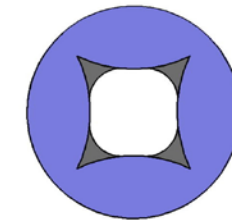
(c)



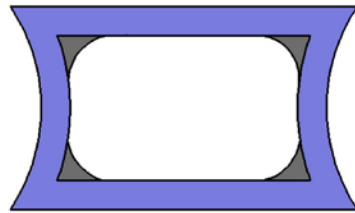
(d)



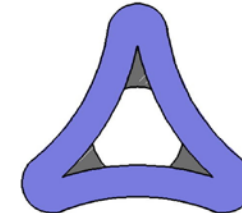
(e)



(f)

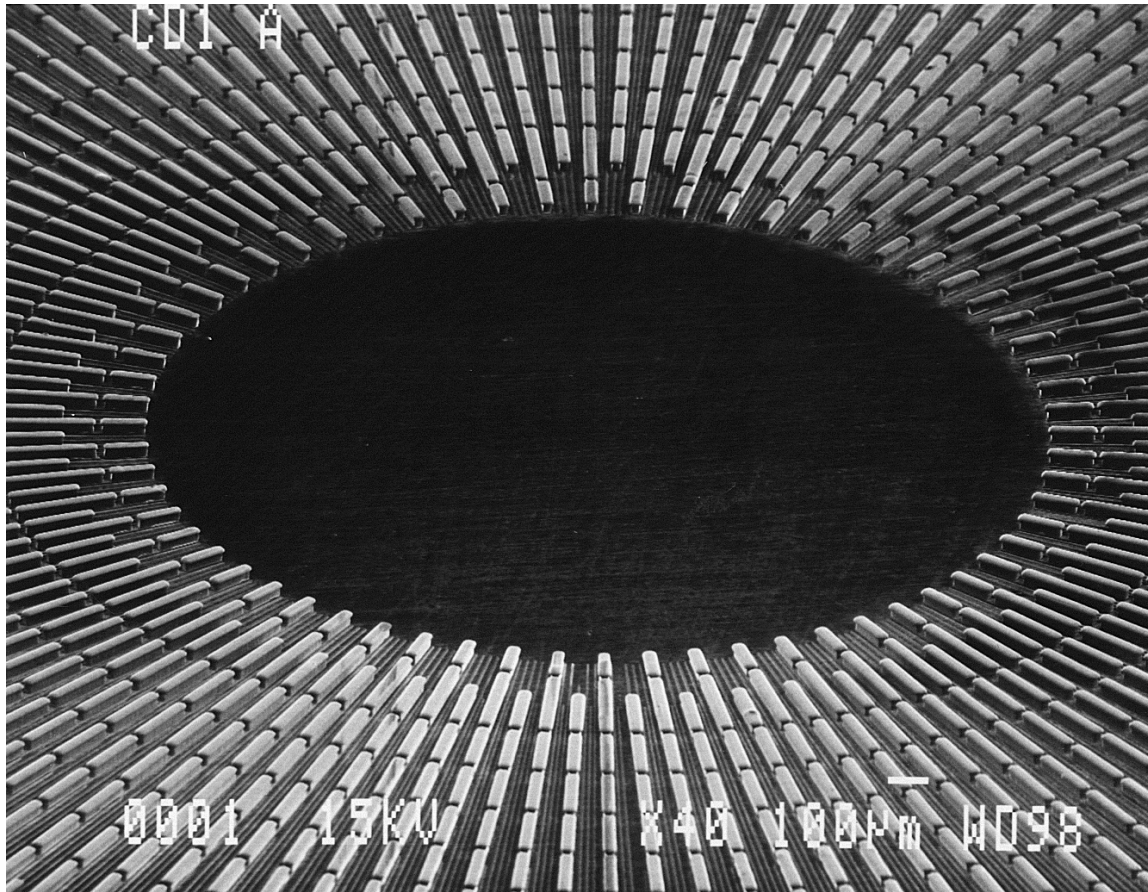


(g)



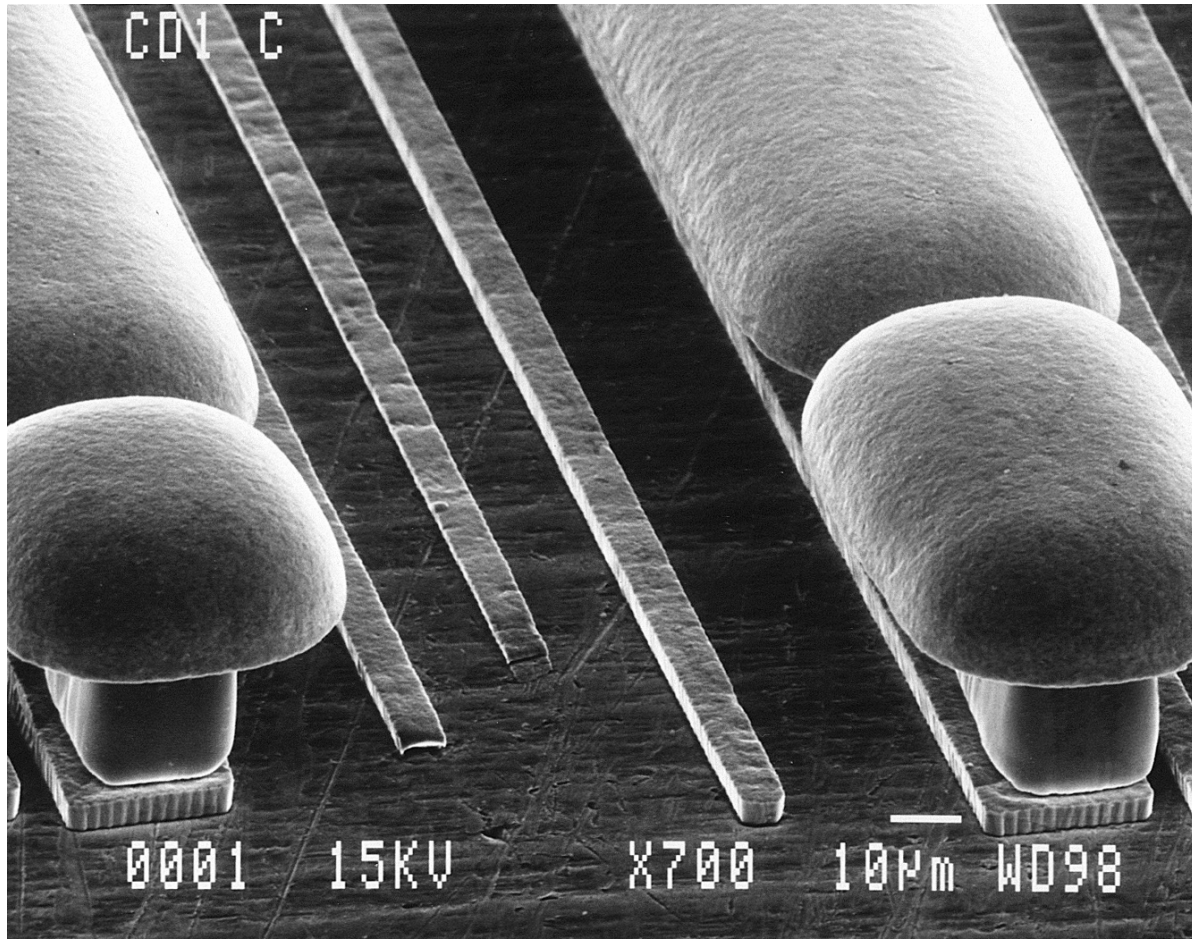
(h)

(a) and (h) triangular section; (b) and (g) rectangular section; (c), (d) and (f) square section; (e) trapezoidal section



Sandia
National
Lab, 2006

Configuration of micron-scale ridges and valleys forms a radial network of passages within the substrate that, when injected with a coolant, efficiently moves heat away from an operating microchip, which would be adhered to the substrate near the center of the array.

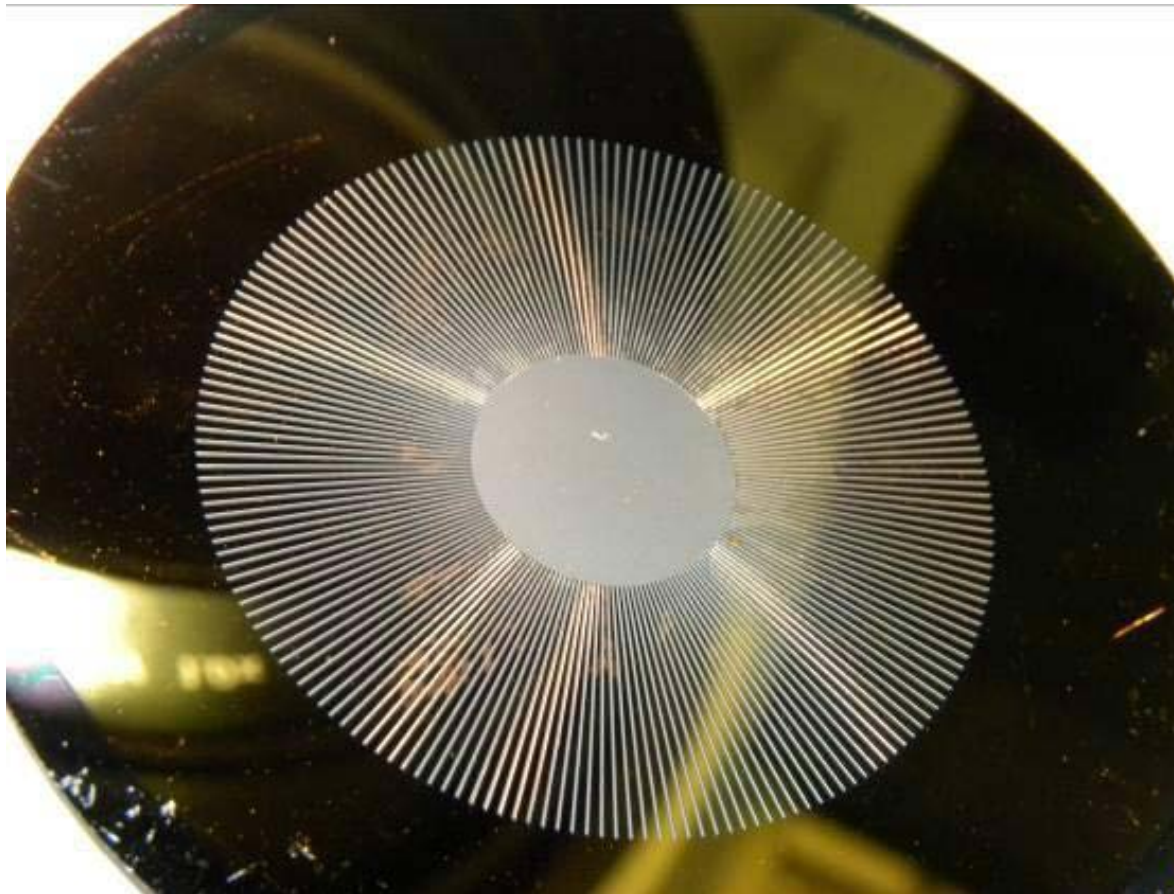


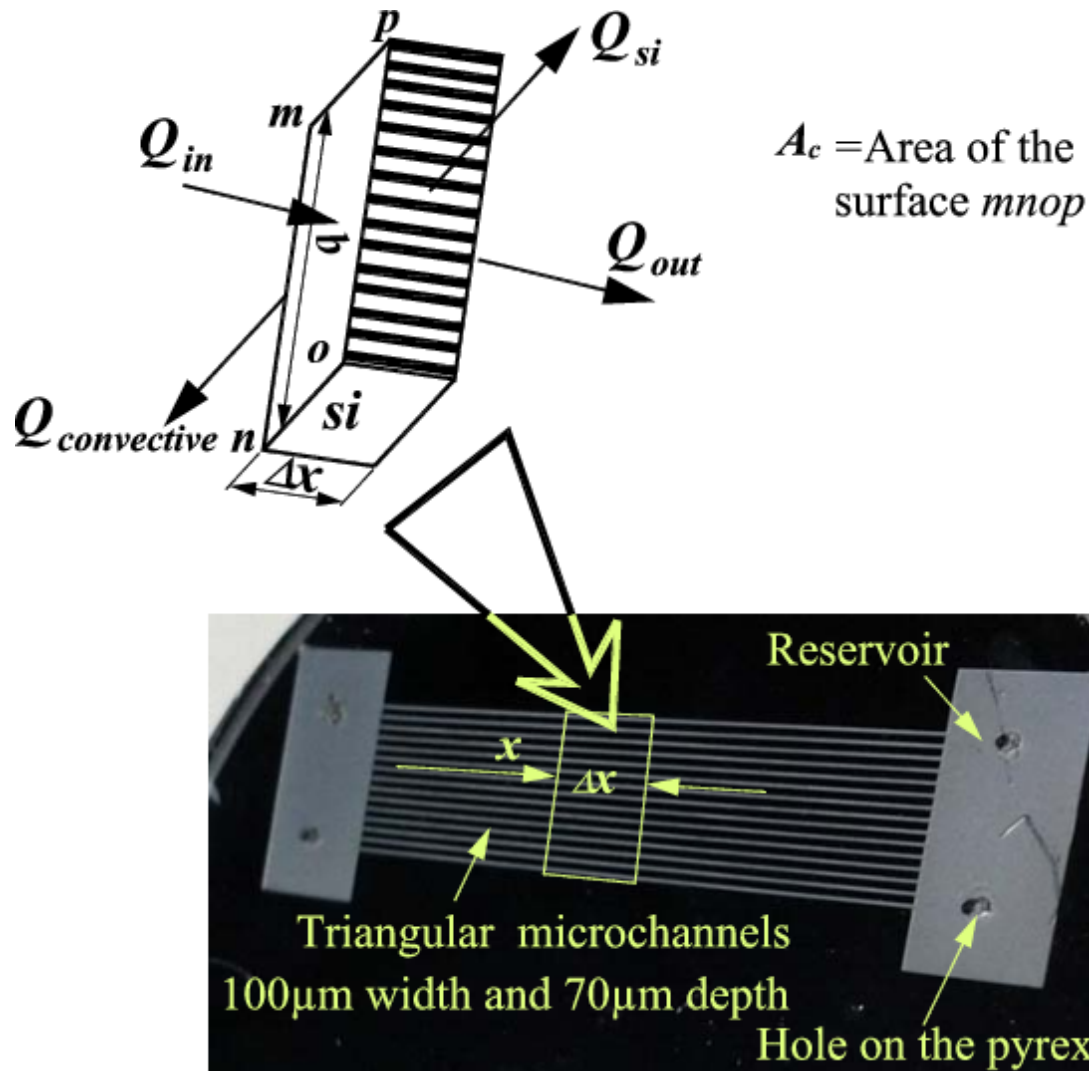
The large ridges are 10-20 microns wide; the smaller are about 5 microns wide

Summary of some typical charging and packaging methods for MEMS-based MHPs.

Working fluids	Charging methods	Volume control	Packaging methods
Methanol	Fully fill working fluid vapor characterized by high pressure and then condense into desired amount of liquid	Accurate	Ionic or ultraviolet bonding
DI water	Fully fill working fluid and then partially remove through evaporation	Less accurate	Sealed with silicone sealant
Ethanol and methanol	Fully fill condensate from working fluid as a vapor and then partially remove through pumping out	Accurate	Sealed with close valve
Water and methanol	Backfill the working fluid after evacuation, and then fill with a micro-metering valve controllably	Accurate	Sealed with close valve
DI water	Fully fill working fluid and then partially remove through pumping out	Less accurate	Fuse the filling glass tube connected to the filling hole

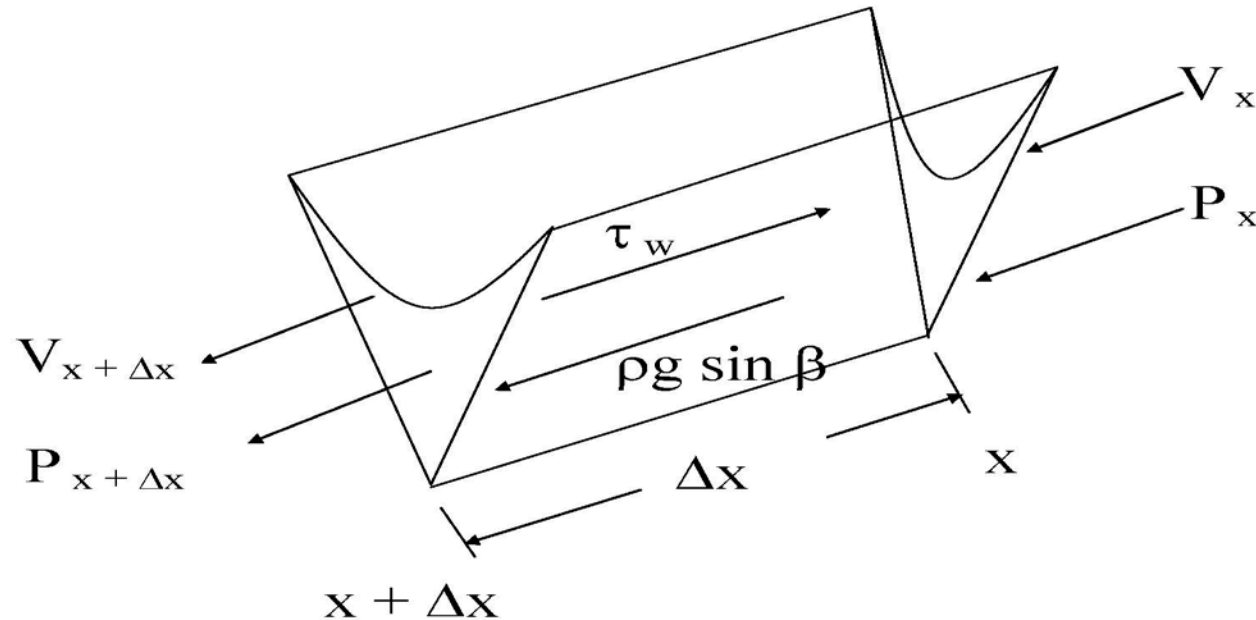
**Radial Grooved U shaped (100 µm x 40 µm)
Microchannel Arrays - RIE
IIT Kharagpur**





Closed microchannel arrays on silicon with reservoirs

Modeling of Flow and Heat Transfer in Microchannels



The liquid pressure as a function of the radius of curvature – from Young-Laplace equation,
$$\frac{dP}{dx} = \frac{\sigma}{R^2} \frac{dR}{dx}$$

$\frac{dP}{dx}$ and $\frac{dR}{dx}$ - pressure and radius of curvature gradient respectively

The steady state momentum balance in differential form

$$\rho A_l V \frac{dV}{dx} + A_l \frac{dP}{dx} + 2 L_h \tau_w - \rho g \sin(\beta) A_l = 0$$

convective momentum pressure force wall shear gravity

A macroscopic approach to develop a general model for a heat pipe with grooves of any shape.

Axial flow due to the change in the radius of curvature.

The effect of body forces incorporated.

Differential form of the mass balance

$$\frac{d}{dx}(\rho V A_l) + \frac{Q_v R_l}{\lambda} = 0$$

Net mass entering the volume element is equal to the mass evaporated from the volume element

Energy balance in the volume element

$$\rho C_p V A_l \frac{dT}{dx} = Q W_b - Q_v R_l$$

Heat supplied to the element is equal to the evaporative heat leaving the element

Boundary Conditions

$$x = 0$$

$$V = 0$$

$$x = L \quad R = R_o$$



$$P = P_{v_o} - \frac{\sigma}{R_o}$$

from geometry for filled groove

$$p_v - p_l = \frac{\sigma}{r}$$

$$\rho \left[\frac{\partial V}{\partial t} + (\bar{V} \cdot \nabla) \bar{V} \right] = -\nabla P + F_B + \mu \nabla^2 \bar{V}$$

Because the flow rate is very small, the convective term in the equation can be neglected

$$\frac{dp_l}{dx} + \rho_l g \sin \beta + F_v = 0,$$

$$\frac{dP_l}{dx} = -\frac{d}{dx}(P_v - P_l) = -\frac{d}{dx}\left(\frac{\sigma}{r(x)}\right)$$

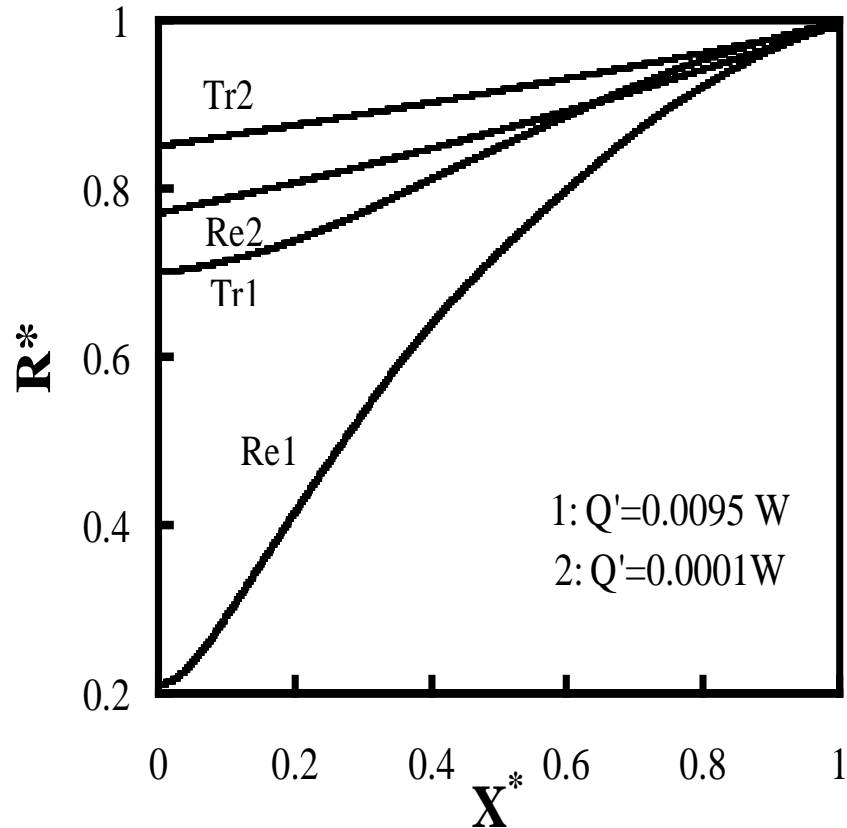
$$\frac{d}{dx} \left(\frac{\sigma}{r(x)} \right) = \left(\frac{2K\mu_l}{c_3 r(x)^4} \right) \Gamma_c + \rho_l g \sin \beta,$$

$$c_3 = 4 \tan^2 \alpha \left(\frac{1}{\tan \alpha} + \alpha - \pi/2 \right)^3.$$

Γ_c , is the mass flow rate through the cross-section of the groove, and the parameter ‘K’ is a function of the groove half angle, a , and the liquid contact angle. Equation is valid for both the evaporative and adiabatic regions

$$\Gamma_c = \int_0^{\Gamma_c} d\Gamma_c = \left(\frac{2\omega_b}{h_{fg}} \right) \int_x^{x_{max}} q''(x) dx.$$

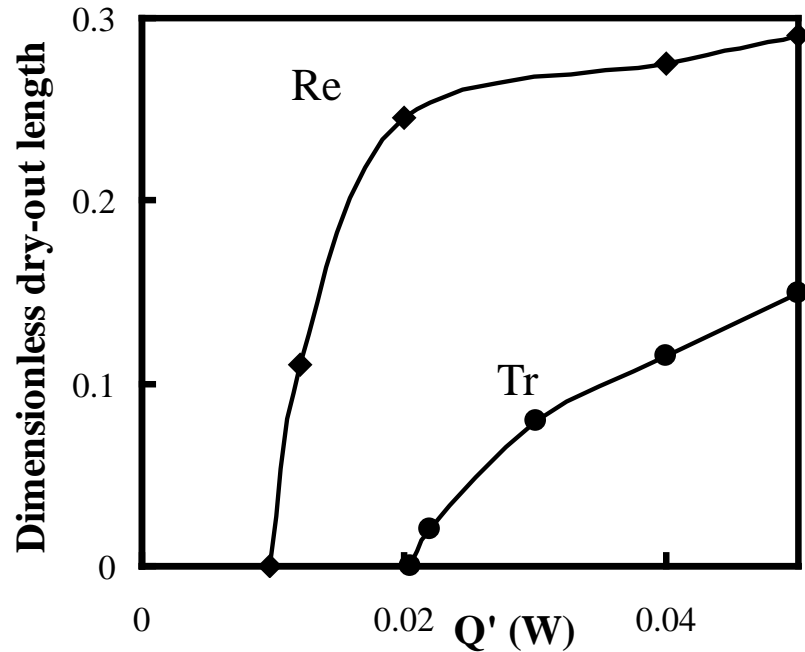
Numerical Solution for two heat pipe geometries – triangular (400 μm side) and rectangular (800 μm x 400 μm)



Profiles of the dimensionless radius of curvature along the length of the heat pipe for different values of heat input and heat pipe geometry

The behavior of the radius of curvature gives a qualitative idea of the capillary pumping capacity

For the same heat input, the liquid meniscus will be more depressed (higher curvature) at the hot end for the case of a rectangular heat pipe compared to a triangular heat pipe.



Variation of the dimensionless dry-out length.

Critical heat input: the flow resulting from the curvature change will not be able to meet the evaporation rate. The radius of curvature at the hot end reaches a value close to zero.

Operating Limits of HP and MHP

Capillary Limit

Working fluid circulation in a heat pipe is achieved through the capillary pressure head developed within the grooves

The capillary pressure head must be greater than the sum of pressure losses along the vapor-liquid path.

The approximate maximum heat transport for steady state (Cotter)

$$Q_{\max} = \frac{0.16\beta \sqrt{K_l K_v}}{8\pi H(1)} \frac{\sigma h_f}{v_l} \sqrt{\frac{v_l}{v_v}} \frac{A^2}{L}$$

Where K_l and K_v are flow shape factors and $H(1)$ is an integral of the fraction of the total heat transport over the length of the pipe, and β is dimensionless geometric factor.

Sonic Limit

The vapor mass flow rate increases with decrease in the condenser pressure.

As the velocity reaches the sonic velocity at the end of the evaporator, further reduction in condenser pressure will not lead to any increase in mass flow rate.

This velocity of vapor is called the sonic limit.

$$Q_{s,\max} = A_v \rho_v h_f \left(\frac{\gamma_v R T_v}{2(\gamma_v + 1)} \right)^{1/2}$$

Where γ is the ratio of specific heats and R is gas constant

Entrainment Limit

Very high vapor velocity in opposite direction may cause waves and the interfacial shear forces may become greater than the liquid surface tension forces.



Entrainment of liquid droplets



Limits axial heat flux

Entrainment limit can be estimated

$$Q_{e,\max} = A_v h_R \left(\frac{\sigma \rho_v}{2r_h} \right)^{1/2}$$

where r_h is the hydraulic radius of the wick structure

Viscous Limit

At low operating temperatures, the vapor pressure difference between the evaporative and the condenser region may be very small.

The viscous forces within the vapor region may actually be larger than the pressure gradients caused by the imposed temperature field.

The no-flow and low flow condition in the vapor portion of a heat pipe is referred to as the viscous limitation.

Most often observed in cryogenic heat pipes.

$$Q_{v,\max} = \frac{r_v^2 h_{fg} \rho_v P_v A_v}{16 \mu_v L_{\text{eff}}}$$

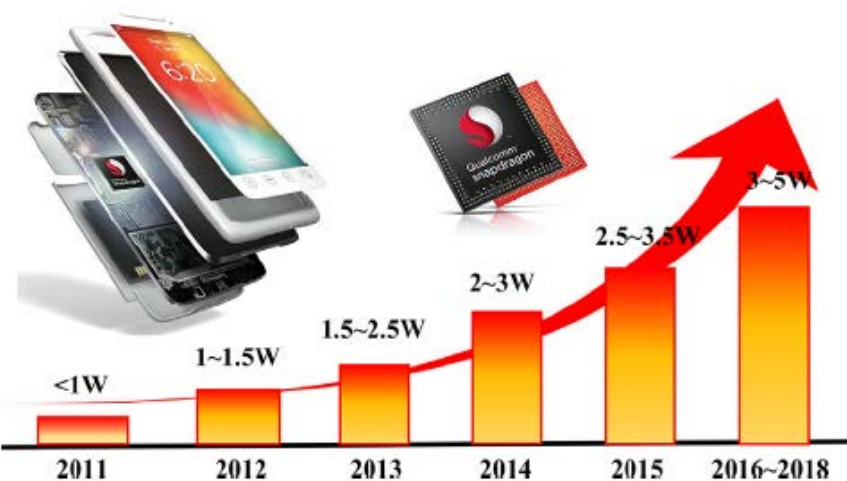
r_v is the equivalent radius of vapor space, L_{eff} effective length of heat pipe.

Major Conclusions

- Effects of body forces are small compared to surface force (true for smaller channels)
- The liquid will be equally distributed among all corners
- Increase in the apex angle reduces capillary suction capability
- The profile of the radius of curvature is used to predict the onset of the dry-out point.
- Dry-out length increases with increase in number of corners, heat input and inclination.

Ultra-thin Micro Heat Pipes for Electronic Cooling

To address the development requirements of mobile electronics,



Power consumption of CPU processors of mobile phones

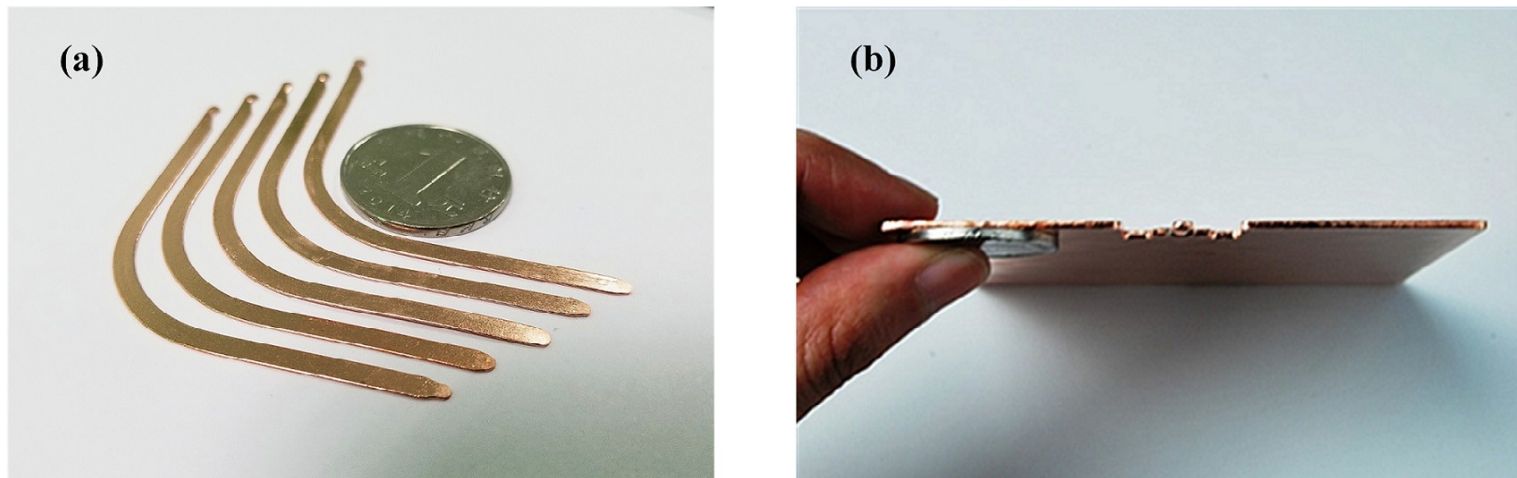
Research in the field of UTHPs has focused on the thickness range 1.0–1.5 mm. However, as the smartphone develops and becomes popularized rapidly, UTHPs with thicknesses below 0.6 mm have become the current research focus.

The rapid development of UTHPs has provided a highly efficient method to cool electronic devices with high power density and limited heat dissipation space.⁶³



Applications of UTHPs in portable electronic devices.

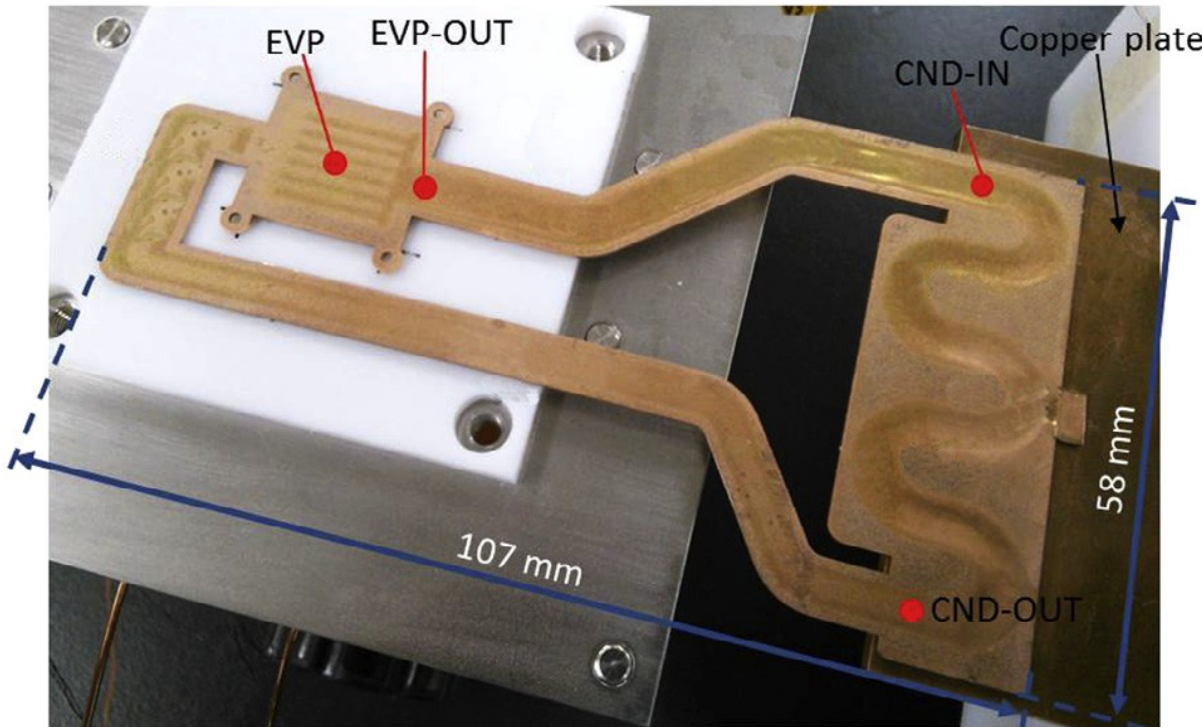
Ultra-thin flat-plate heat pipes



Images of UFHPs: (a) flattened heat pipe and (b) vapor chamber

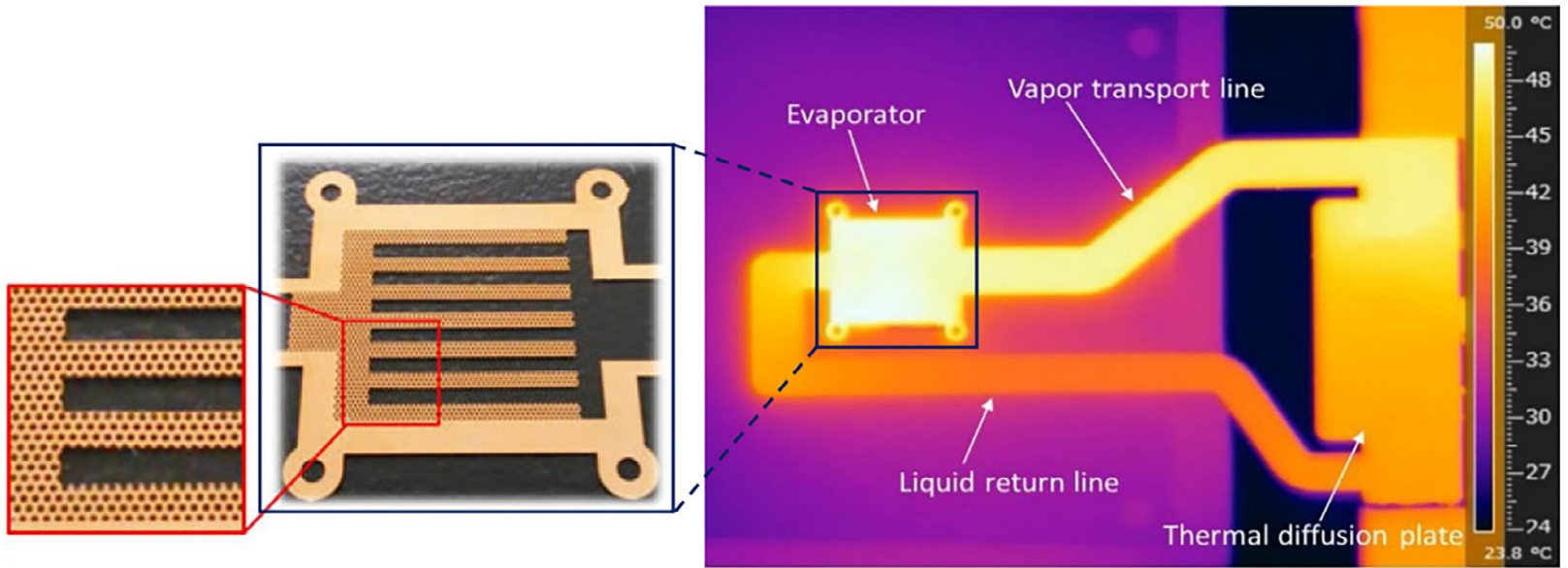
A flat-plate heat pipe is a chamber of low thickness filled with a two-phase working fluid. It can be divided into flattened heat pipes (FHPs) and vapor chambers (VCs) based on the packaging forms. The FHPs are fabricated by flattening conventional cylindrical heat pipes directly, and the composition and operational principles are similar to that of the micro heat pipes,

Ultra-thin loop heat pipes



ULHP for the thermal management of a mobile phone

The loop heat pipe (LHP) is widely utilized for thermal control of electronic equipment in various fields from aerospace to terrestrial industries. LHPs possess certain unique features such as long heat transport distances, lower thermal resistance, reliable operation against gravity and design flexibility.⁶⁶



Wick structure of evaporator section and infrared image of steady state operation of ULHP

Interfacial Phenomena in a Thin Film

MOTIVATION

- Interfacial phenomena involve the study of
 - Capillary forces
 - Marangoni stresses (flow due to surface tension gradient)
 - Liquid/Vapor Interfacial Phase-Change
 - Intermolecular forces (van der Waals interactions, etc.)
 - These concepts are important in explaining fundamental phenomena like spreading, coating, adsorption, stability, pattern formation, evaporation, condensation, etc.
-

MOTIVATION : APPLICATIONS

1. Miniature Heat Pipes

Passive fluid flow and phase-change heat transfer
(evaporation and condensation)

2. Surfactant adhesion/spreading

Spreading of surfactant containing drops

3. MEMS/Microfluidics

Fluid flow and phase-change in micro-channels, droplets

4. Micro-electronics

Stability of thin solid films on Si, adhesive properties of
thin porous films for spin coating applications etc.

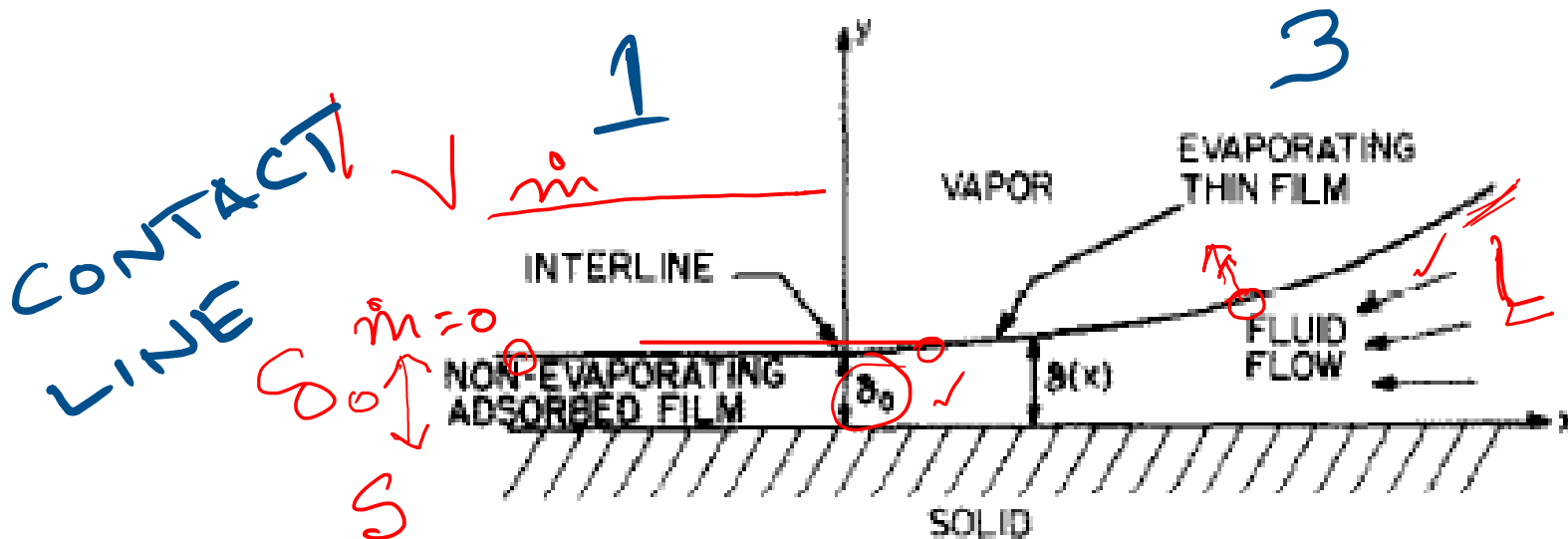


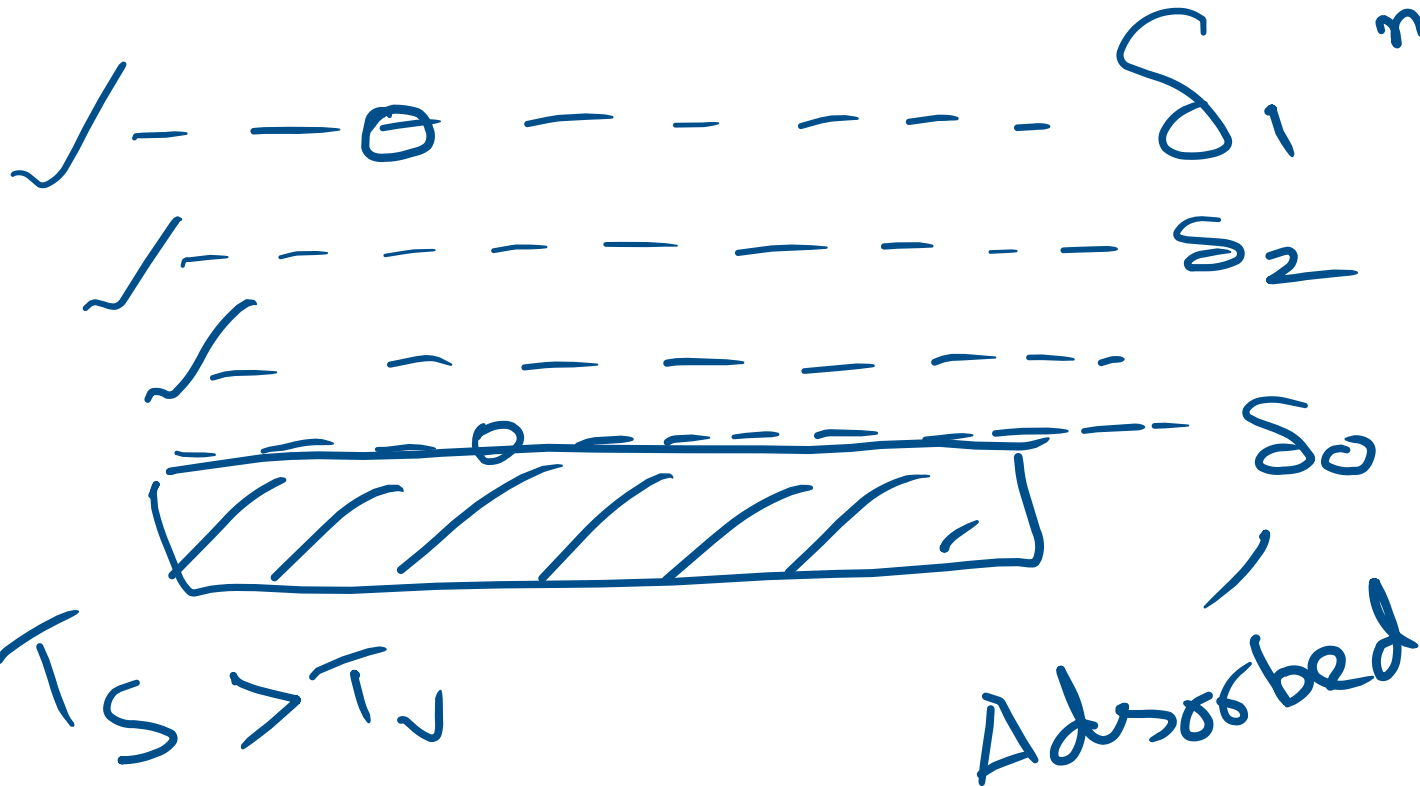
FIG. 1. Interline junction of vapor, adsorbed evaporating thin film and adsorbed non-evaporating thin film.

The heat transfer and other transport phenomena in the **contact line** (interline) region, where the liquid, vapor and the solid are in close proximity are important in many technologically important processes, e.g., rewetting of a hot spot.

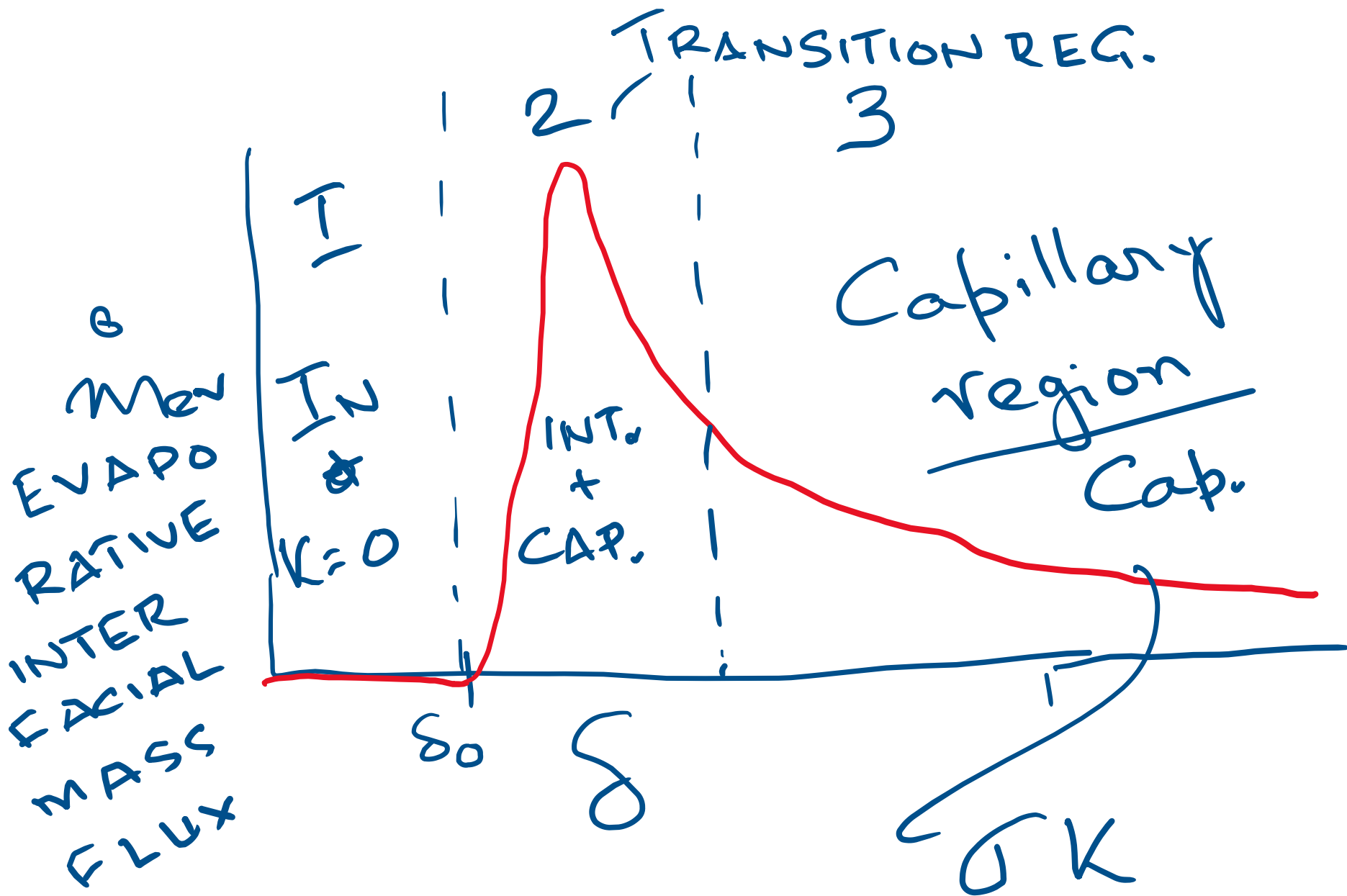
$$F_d \leq \frac{\bar{A}}{S_n}$$

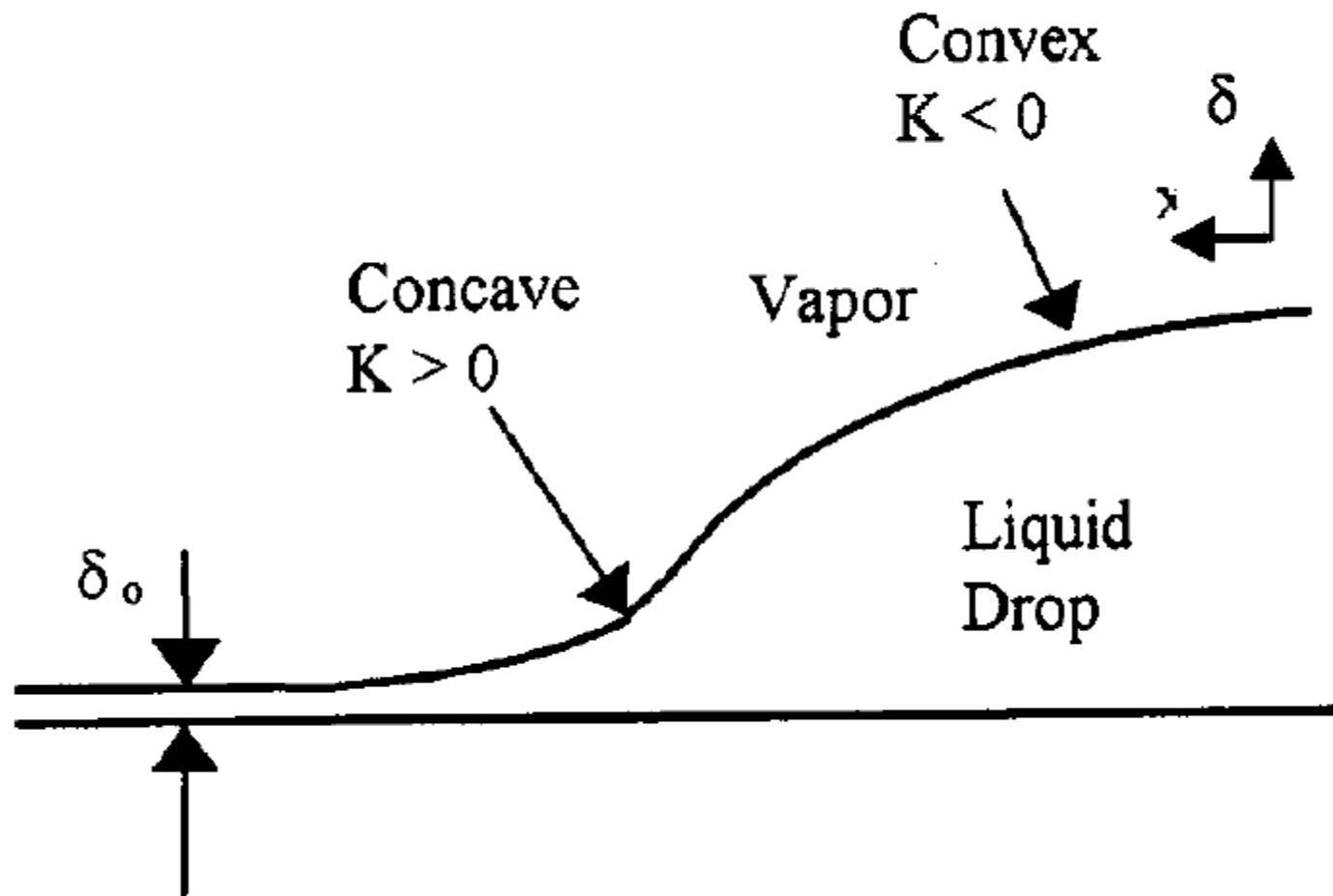
$n=3, 4$

T_N



$T_S > T_N$





Schematic drawing of the measured interfacial profile of a condensing drop

INTRODUCTION

Capillary Pressure : $\sigma_{1v} K$

K is the curvature,
+ve for a concave surface,
-ve for a convex surface

Disjoining pressure :

$$\Pi = \frac{-\bar{A}}{\delta^3} ; \quad \text{Red note: } \bar{A} = P/16\pi$$

$$= -\frac{B}{\delta^4} ; \quad \delta > 20nm$$

\bar{A} is the modified Hamaker constant,
B is the dispersion constant

They are negative for a wetting system

Capillary and disjoining pressures are functions of the thickness profile.

Augmented Young-Laplace equation

$$\Delta P = P_l - P_v = -\sigma K - \Pi$$

where P_v is the vapor pressure, P_l is the pressure inside the liquid, K is the curvature of the liquid–vapor interface, σ is the surface tension, and δ is the film thickness of the liquid.

The second term on the right-hand side of the equation signifies the van der Waals interactions and is defined as⁴⁹

$$\frac{\partial \Delta G^{vdw}}{\partial \delta} = \frac{A}{6\pi\delta^3} = -\Pi,$$

Where ΔG^{vdw} is the excess interfacial free energy per unit area due to the van der Waals interactions. It includes the contributions from dipolar interactions (purely entropic) and dispersion energy. The symbol A is the Hamaker constant

A negative value of the Hamaker constant (van der Waals interaction) signifies that a thin film in the microscopic region, with a thickness of that studied herein, will be stable and will reduce the free energy of the system.

We use the sign convention that a negative Hamaker constant and a positive disjoining pressure (Π) represent a system showing a stable, adsorbed wetting film.

The Hamaker constant, A, for two phases, 1 and 2, interacting across a medium 3 can be expressed in terms of the refractive indices and the dielectric constants of the three phases.

$$A = \frac{3}{4} kT \left(\frac{\varepsilon_1 - \varepsilon_3}{\varepsilon_1 + \varepsilon_3} \right) \left(\frac{\varepsilon_2 - \varepsilon_3}{\varepsilon_2 + \varepsilon_3} \right) + \frac{3h\nu_e}{8\sqrt{2}} \frac{(n_1^2 - n_3^2)(n_2^2 - n_3^2)}{(n_1^2 + n_3^2)^{1/2}(n_2^2 + n_3^2)^{1/2}\{(n_1^2 + n_3^2)^{1/2} + (n_2^2 + n_3^2)^{1/2}\}},$$

where ε is the static dielectric constant, k is the Boltzmann's constant, h is the Planck's constant, ν_e is the plasma frequency of the free electron gas and n is the refractive index.

INTERFERENCE + ELLIPSOMETRY

$S(\lambda)$

S_{0th} dark
 S_{0th}

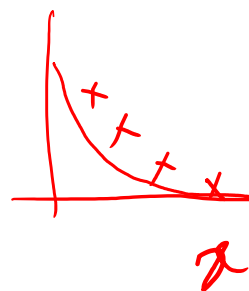
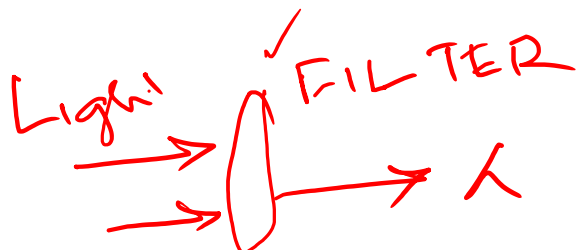
1st bright
fringe

~~known~~
 $f^*(S, n_r, \lambda)$



$0.01, 0.3, 0.5$

Typical interference pattern observed for heptane on glass



Langmuir 2007, 23, 1234–1241

Force field characterization model

$$\Pi + \sigma K - \rho_l g H = 0 \quad \text{Force balance at equilibrium}$$

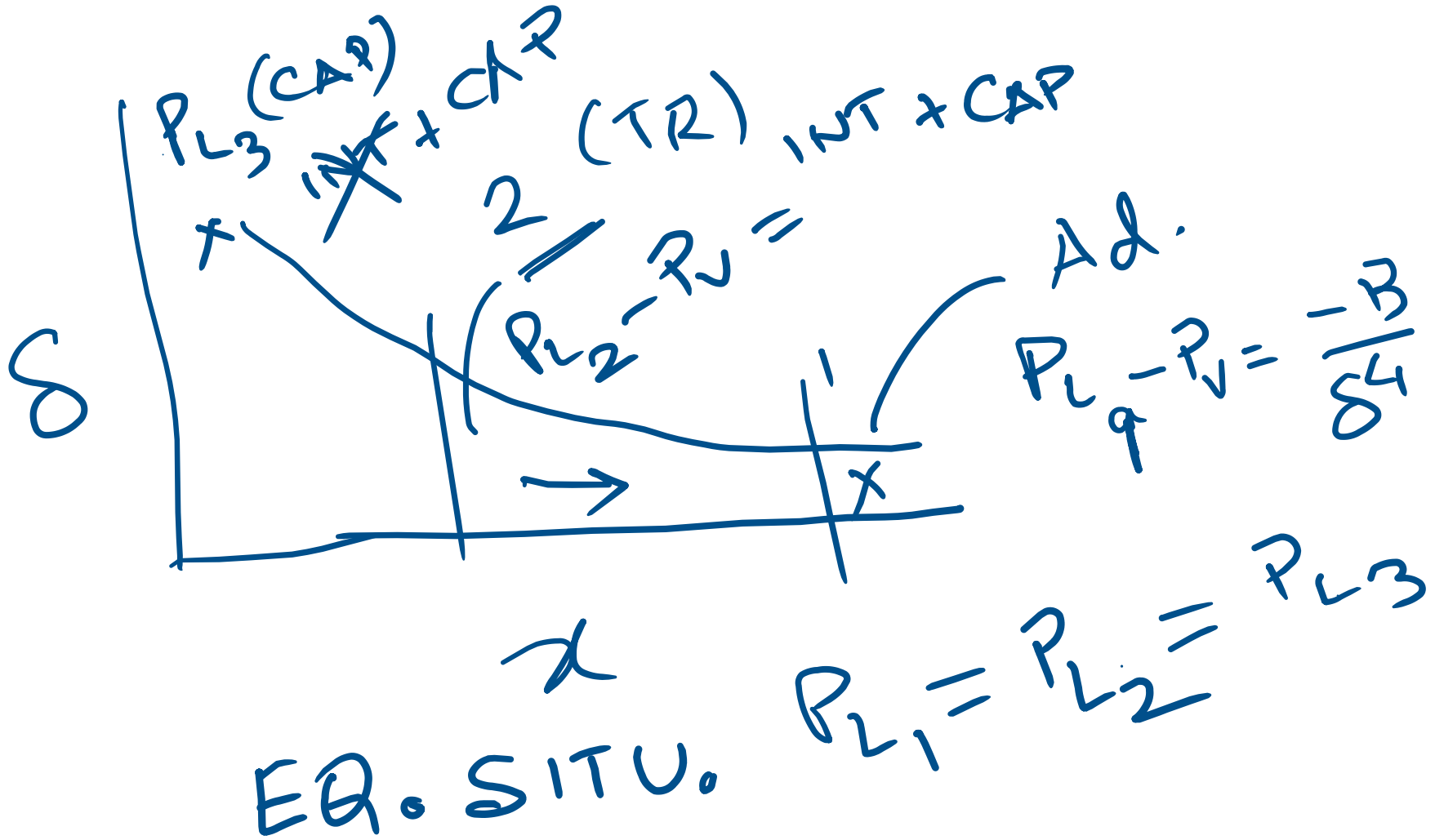
$$\Pi(\text{Disjoining Pressure}) = \frac{-B}{\delta^n} \quad \text{Disjoining pressure}$$

$$\Delta P = P_l - P_v = -\sigma K - \Pi \quad \text{Augmented Y-L equation}$$

$$\sigma K - \frac{B}{\delta^4} = \sigma K_\infty \quad Q = 0$$

Isothermal condition, K_∞ is the curvature of the capillary meniscus

$$\sigma \frac{d^2 \delta}{dx^2} - \frac{B}{\delta^4} = \sigma K_\infty \quad \text{Using simplified form of curvature}$$



Non-dimensionalization

$$\eta = \frac{\delta}{\delta_0} \quad Z = x \left(\frac{K_\infty}{\delta_0} \right)^{1/2}$$

$$\frac{d^2\eta}{dZ^2} + \left(\frac{-B}{\sigma K_\infty \delta_0^4} \right) \frac{1}{\eta^4} = 1.$$

Parameter, α ,
defined as

$$\alpha^4 = \frac{-B}{\sigma K_\infty \delta_0^4}$$

α is a measure of the deviation of a specific meniscus from the equilibrium conditions, $\alpha = 1$ at equilibrium

$$\left(\frac{d\eta}{dZ} \right)^2 = 2\eta + \frac{2}{3} \frac{\alpha^4}{\eta^3} + C_1 \rightarrow$$

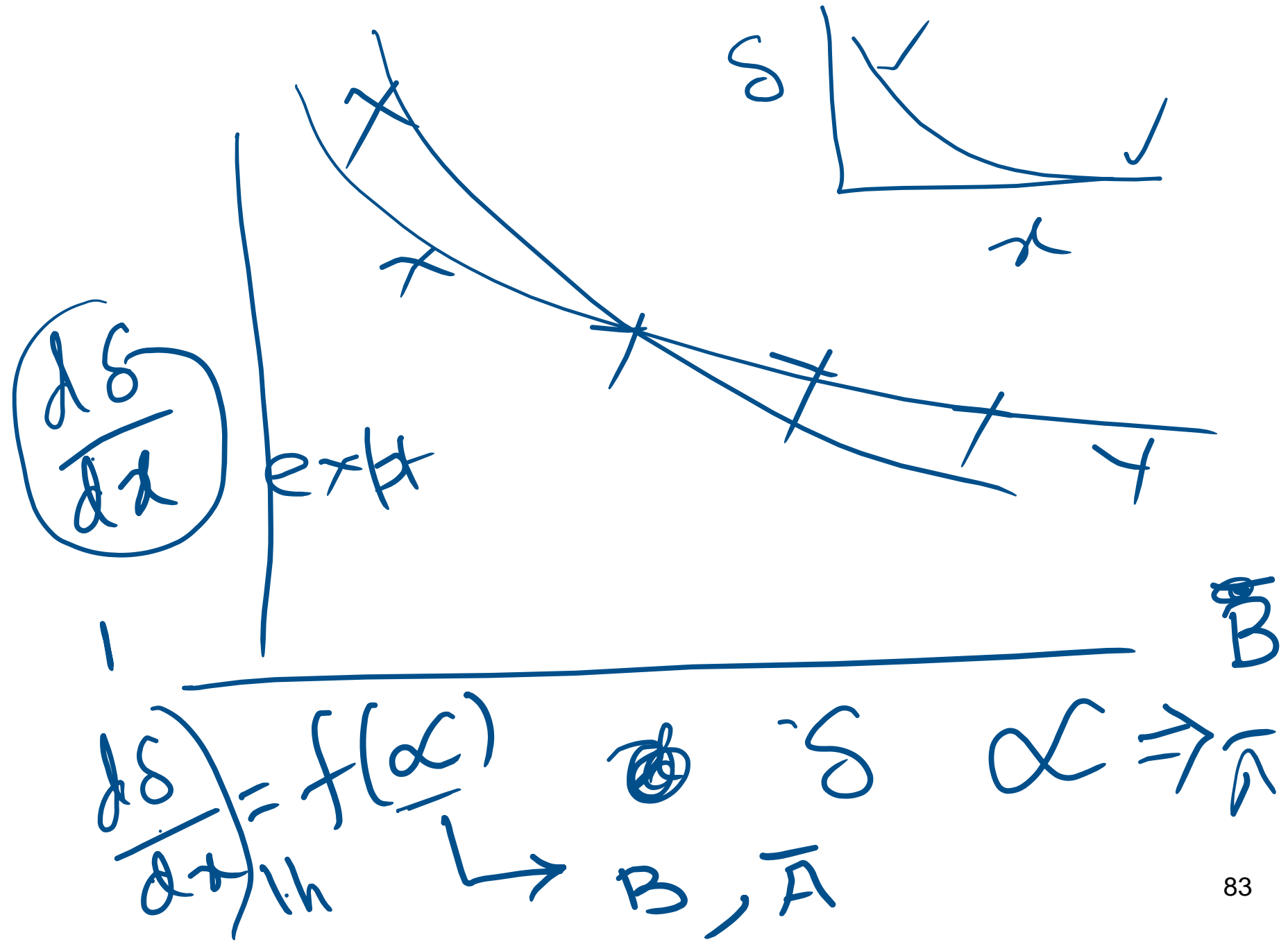
BC

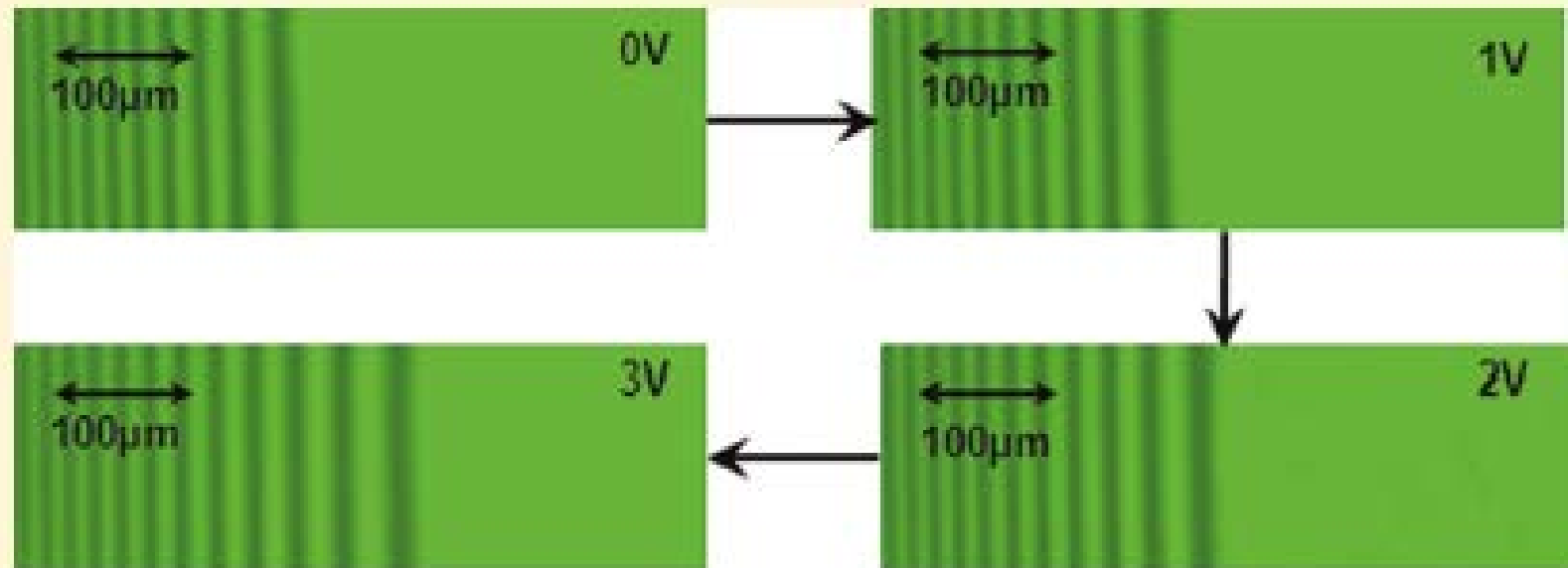
$$\eta = \alpha, \frac{d\eta}{dZ} = 0,$$

Slope of a curved thin film can be obtained accurately using Y-L eqn.

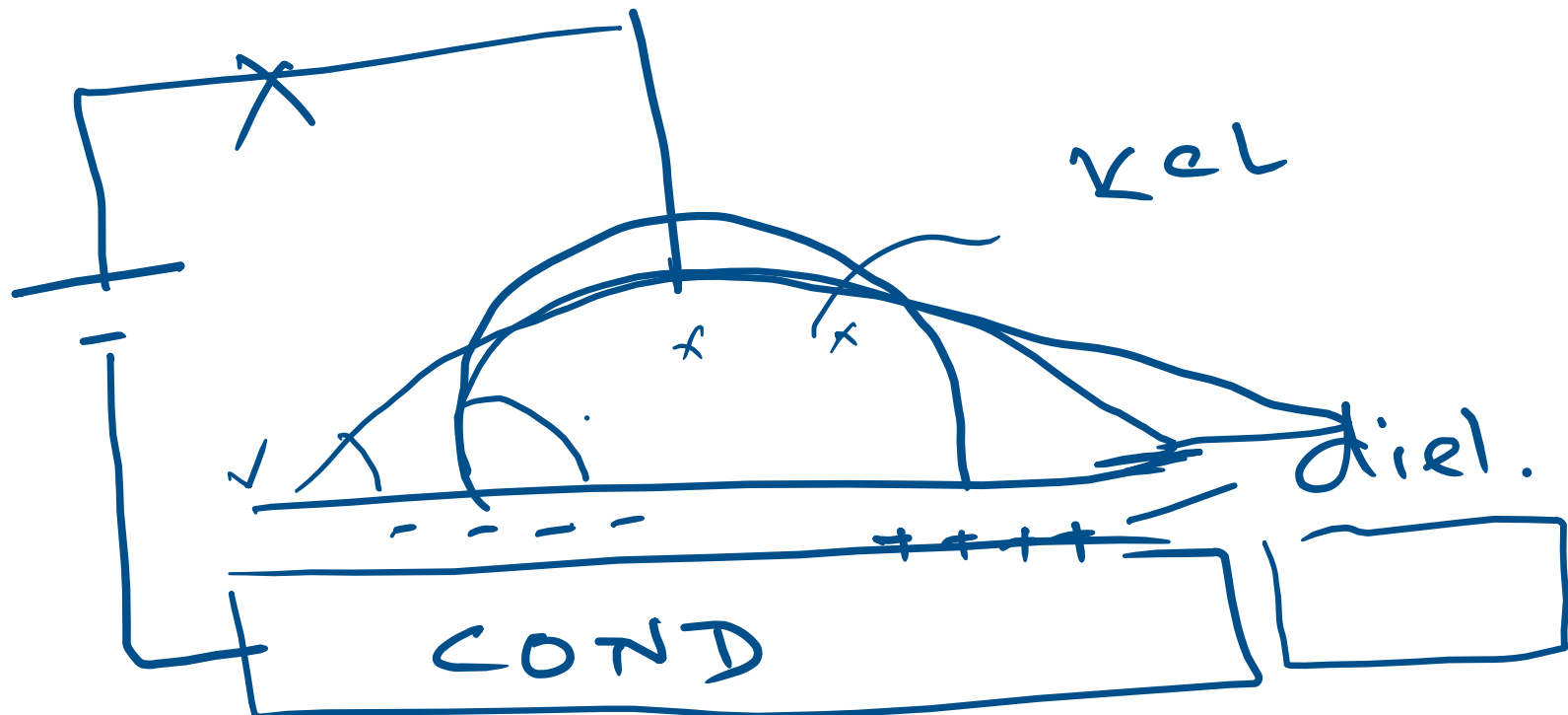
$$\frac{d\delta}{dx} = -(K_\infty \delta_0)^{1/2} \sqrt{2\eta + \frac{2}{3} \frac{\alpha^4}{\eta^3} - \frac{8}{3}\alpha}$$

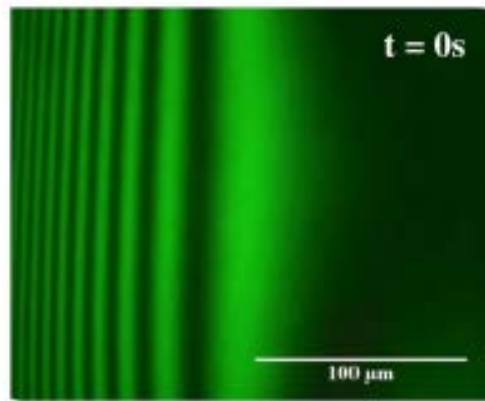
IN-SITU evaluation of B



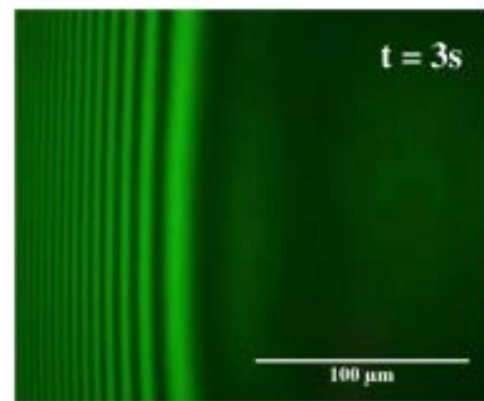


Spreading of a surfactant (0.1 CMC SDS) laden thin water film on a SiO_2 substrate on application of electric field (0-3V)

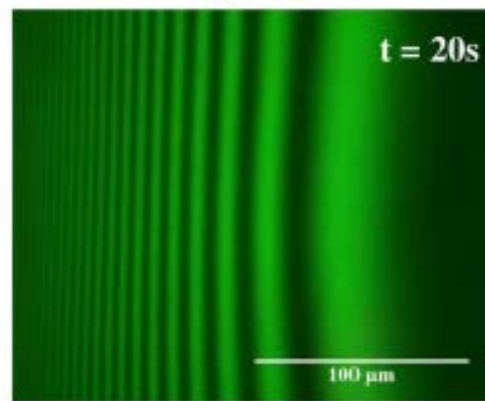




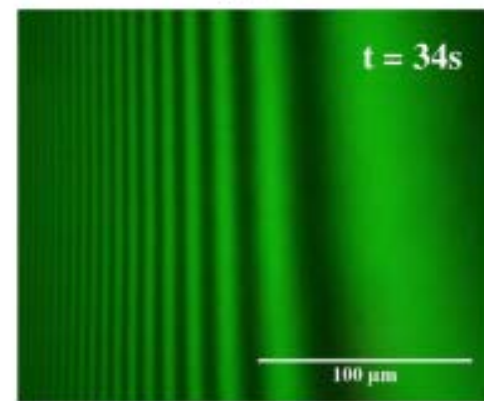
(a)



(b)



(c)



(d)

Image sequence depicting the dynamics of the thin film when subjected to a magnetic field